

A closed-form solution for composite tunnel linings in a homogeneous infinite isotropic elastic medium

Hany El Naggar, Sean D. Hinchberger, and K.Y. Lo

Abstract: This paper presents a closed-form solution for composite tunnel linings in a homogeneous infinite isotropic elastic medium. The tunnel lining is treated as an inner thin-walled shell and an outer thick-walled cylinder embedded in linear elastic soil or rock. Solutions for moment and thrust have been derived for cases involving slip and no slip at the lining–ground interface and lining–lining interface. A case involving a composite tunnel lining is studied to illustrate the usefulness of the solution.

Key words: thin-walled shell, thick-walled cylinder, moment, thrust, tunnel lining, plane strain solution.

Résumé : Cet article présente une solution exacte des garnitures de tunnels composites dans un milieu élastique isotrope infini homogène. La garniture de tunnel est traitée comme une coquille intérieure à paroi mince et un cylindre extérieur à paroi épaisse dans un sol élastique linéaire ou un roc. Les solutions pour le moment et la pression ont été dérivées pour le cas impliquant du glissement ou non à l'interface garniture–sol et garniture–garniture. On étudie un cas impliquant une garniture de tunnel composite pour illustrer l'utilité de la solution.

Mots-clés : coquille à paroi mince, cylindre à paroi épaisse, moment, pression, garniture de tunnel, solution à déformation plane.

[Traduit par la Rédaction]

Introduction

Many cities rely on tunnels for transportation, water distribution, and sewage handling. Consequently, these structures have high social and economical value. In some cases, long-term exposure of a reinforced concrete lining to sulphates or chlorides in groundwater can lead to concrete deterioration and consequent reduction in the load carrying capacity of the lining. For this situation, engineers may be required to estimate the distribution of moment and thrust in the degraded liner to evaluate its factor of safety. Closed-form solutions can be economical for such applications especially if liner degradation is widespread in a tunnel system of variable depth.

Many closed-form solutions have been developed to estimate the distribution of moment and thrust in tunnel supports (e.g., Morgan 1961; Muir Wood 1975; Rankine et al. 1978; Einstein and Schwartz 1979; Yuen 1979). However, none of these solutions account for composite linings such as those shown in Fig. 1 nor do they account for the initial stress relief that can occur due to ground convergence prior to installation of the liner (e.g., Lee et al. 1992). Only Lo and Yuen (1981) have accounted implicitly for ground convergence prior to installation of the liner; however, their solution is for a single tunnel lining embedded in a viscoelastic medium. Ogawa

(1986) has studied composite tunnel linings comprising inner and outer thick-walled cylinders embedded in an infinite elastic medium. However, this solution (Ogawa 1986) is not easily applied to segmental concrete tunnel linings, and it also does not account for stress relief prior to liner installation. Table 1 summarizes some of the existing closed-form solutions.

This paper presents a new closed-form solution for composite tunnel liners embedded in an infinite elastic medium (see Fig. 2). In the solution, the lining system is idealized as an inner thin-walled shell and an outer thick-walled cylinder. The ground is treated as an infinite elastic medium governed by Hooke's law, and the principle of superposition is used to approximately account for the impact of some initial ground convergence during construction on the moments and thrusts mobilized in the liner system. The solution applies to tunnels in intact rock or strong soils that remain predominantly elastic during tunnel construction. Its advantages are: (i) that it is easier to apply to cases involving segmental concrete tunnel linings, and (ii) that it can be used to approximately account for partial closure of the gap (Lee et al. 1992) prior to lining installation. The solution, which is considered to be a new and useful tool for tunnel engineers, is used to study the impact of a thick-grouted annulus on moments and thrusts in a segmental concrete tunnel lining.

Received 7 August 2006. Accepted 31 January 2007. Published on the NRC Research Press Web site at cgj.nrc.ca on 14 March 2008.

H. El Naggar, S.D. Hinchberger,¹ and K.Y. Lo. Geotechnical Research Centre, Department of Civil and Environmental Engineering, The University of Western Ontario, London, ON N6A 5B9, Canada.

¹Corresponding author (e-mail: shinchberger@eng.uwo.ca).

Fig. 1. Common double lining systems.

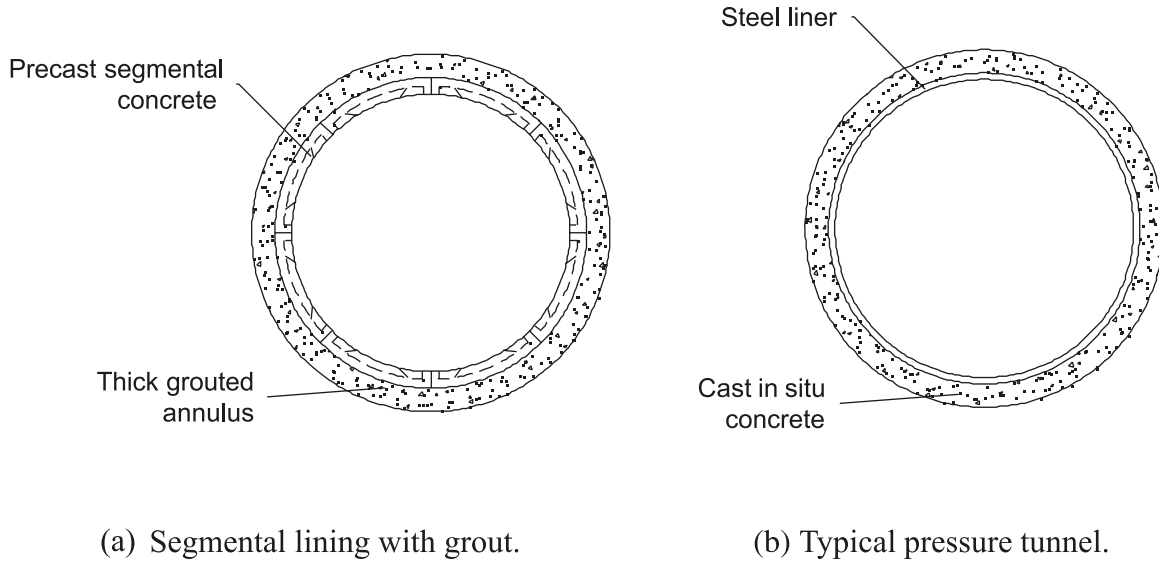


Table 1. Comparison of closed-form solutions for circular tunnels in elastic ground.

Solution	Stress function	Liner idealization	Joints	Gap closure
Morgan (1961)	Airy	Thin-walled tube	Easy: by reducing I_{liner}	No provision
Muir Wood (1975)	Airy	Thin-walled tube	Easy: by reducing I_{liner}	No provision
Einstein and Schwartz (1979)	Mitchell	Thin-walled shell	Easy: by reducing I_{liner}	No provision
Yuen (1979)	Airy	Thick-walled cylinder	Possible: by reducing the liner thickness and adjusting E	No provision
Ogawa (1986)	Airy	Inner and outer thick-walled cylinders	Possible: by reducing the liner thickness and adjusting E	No provision

Note: I_{liner} , moment of inertia of the lining; E , Young's modulus.

Problem definition

Figure 2 shows the problem geometry. Solutions for moment, thrust, stress, and displacement are derived in terms of the angle θ measured counterclockwise from the spring line axis of the tunnel. In this paper, the circular tunnel is assumed to be embedded in a homogenous infinite elastic medium subject to an initial anisotropic stress field. The initial vertical and horizontal stresses in the ground are σ_v and σ_h , respectively, where $\sigma_h = K_o \sigma_v$ and K_o is the coefficient of lateral earth pressure at rest. For the solution, the initial stress field (see Fig. 3) is separated into a hydrostatic component, P_o , and deviatoric component, Q_o .

$$[1a] \quad P_o = (\sigma_v + \sigma_h)/2$$

and

$$[1b] \quad Q_o = (\sigma_h - \sigma_v)/2$$

Since tunnels are long linear structures, plane strain conditions have been assumed. The mechanical properties of the ground are assumed to obey Hooke's law with elastic modulus E_g and Poisson's ratio ν_g . The outer lining is treated as a thick-walled cylinder with elastic modulus E_2 , Poisson's ratio ν_2 and inner (intrados) and outer (extrados) radii R_2 and R_3 , respectively. The inner lining is treated as

a thin-walled shell with elastic modulus E_1 , Poisson's ratio ν_1 , cross-sectional area A_1 , and moment of inertia I_1 . The intrados and extrados of the inner lining are defined by R_1 and R_2 , respectively. Excavation of the tunnel is assumed to cause a reduction of the boundary stresses around the circumference of the opening at $r = R_3$ until the new boundary stresses reach equilibrium with the liner reactions. The following sections present the derivation of moments and thrust in a composite tunnel lining for the case of no slip at $r = R_2$ and $r = R_3$. Solutions for slip and no slip at $r = R_2$ and $r = R_3$, respectively, and full slip at both $r = R_2$ and $r = R_3$ are also included.

Stresses and displacements in the ground due to full stress relief

There are several solutions for the distribution of stresses and displacements in an infinite elastic medium due to full stress relief (see Table 1). These solutions typically employ some form of stress function in conjunction with Hooke's law and the equilibrium equations. For example Timoshenko and Goodier (1969) and Einstein and Schwartz (1979) used Mitchell's stress function in their solution; whereas, Morgan (1961), Muir Wood (1975), Yuen (1979), and Ogawa (1986) employed Airy's stress function. In this paper, solutions based on Airy's stress function are utilized.

Fig. 2. Problem geometry – composite lining.

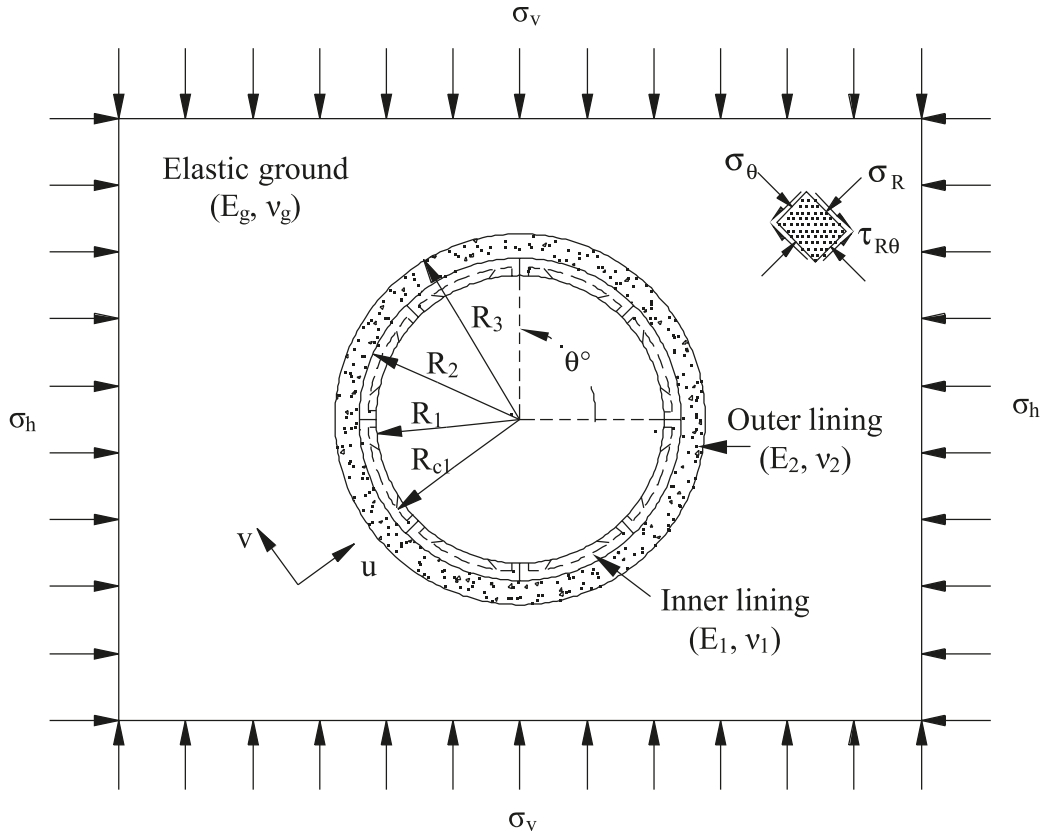
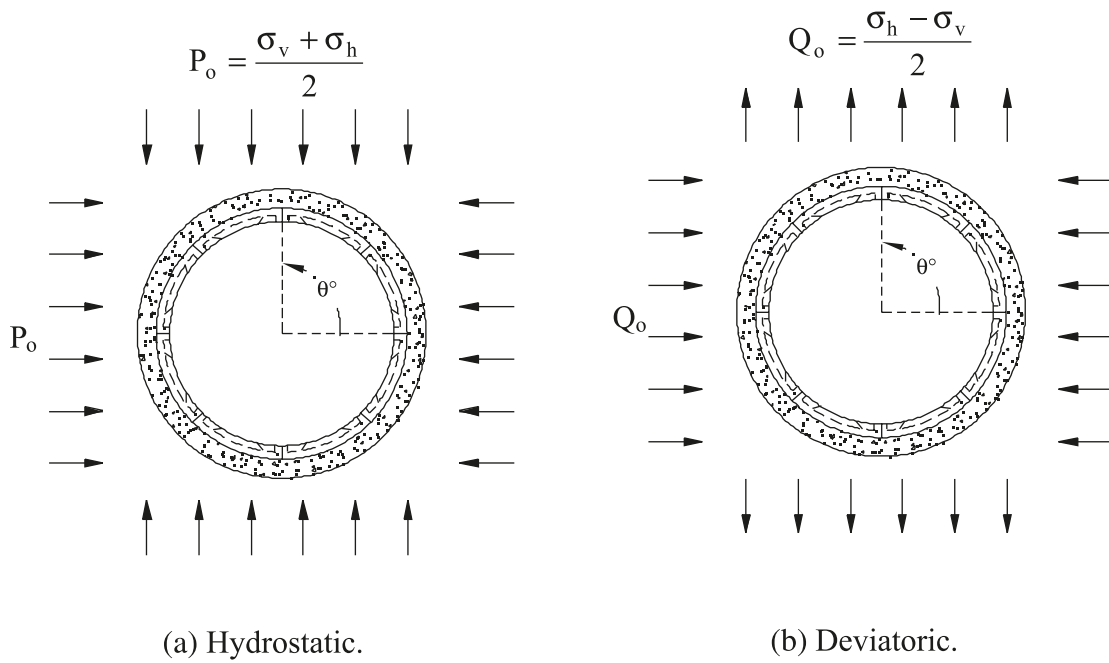


Fig. 3. Hydrostatic and deviatoric components of the initial stress field.



Hydrostatic component, P_o

Considering the hydrostatic component, P_o , the Airy’s stress function is

$$[2] \quad \Phi^H = Ar^2 + C \ln r$$

where r is the radial distance from the longitudinal tunnel axis. From the equilibrium equations, the change in radial, tangential, and shear stress in the ground is given by

$$[3a] \quad \Delta\sigma_R^H = \frac{1}{r} \frac{\partial\Phi}{\partial r} = 2A + \frac{C}{r^2}$$

$$[3b] \quad \Delta\sigma_\theta^H = \frac{\partial^2\Phi}{\partial r^2} = 2A - \frac{C}{r^2}$$

and

$$[3c] \quad \Delta\tau_{R\theta}^H = -\frac{\partial}{\partial r} \left(\frac{1}{r} \frac{\partial\Phi}{\partial r} \right) = 0$$

where the coefficients A and C are determined from suitable boundary conditions (see Appendix A).

From Yuen (1979), the radial deformation in the ground due to the excavation and consequent full stress relief is, from Hooke’s Law,

$$[4] \quad u_g^H = \int \varepsilon_r dr = \frac{P_o(1 + \nu_g)R_3^2}{E_g r}$$

and the stress field in the ground is

$$[5a] \quad \sigma_{Rg}^H = \sigma_{r0} + \Delta\sigma_r = P_o \left[1 - \left(\frac{R_3}{r} \right)^2 \right]$$

$$[5b] \quad \sigma_{\theta g}^H = \sigma_{\theta 0} + \Delta\sigma_\theta = P_o \left[1 + \left(\frac{R_3}{r} \right)^2 \right]$$

and

$$[5c] \quad \tau_{R\theta g}^H = 0$$

Deviatoric component, Q_o

Considering full stress relief of the deviatoric component, Q_o , the Airy’s stress function is

$$[6] \quad \Phi^D = \left[Ar^2 + Br^4 + \frac{C}{r^2} + D \right] \cos 2\theta$$

and again utilizing the equilibrium equations, the change in radial and tangential stresses is given by

$$[7a] \quad \Delta\sigma_{Rg}^D = \frac{1}{r} \frac{\partial\Phi^D}{\partial r} + \frac{1}{r^2} \frac{\partial^2\Phi^D}{\partial\theta^2} = - \left[2A + 6\frac{C}{r^4} + 4\frac{D}{r^2} \right] \cos 2\theta$$

$$[7b] \quad \Delta\sigma_{\theta g}^D = \frac{\partial^2\Phi^D}{\partial r^2} = \left[2A + 12Br^2 + 6\frac{C}{r^4} \right] \cos 2\theta$$

and

$$[7c] \quad \Delta\tau_{R\theta g}^D = -\frac{\partial}{\partial r} \left(\frac{1}{r} \frac{\partial\Phi^D}{\partial r} \right) = \left(2A + 6Br^2 - 6\frac{C}{r^4} - 2\frac{D}{r^2} \right) \sin 2\theta$$

where the coefficients, A , B , C , and D are determined from the boundary conditions; $\Delta\sigma_R = -Q_o \cos 2\theta$ and $\Delta\tau_{R\theta} = Q_o \sin 2\theta$ at $r = R_3$ and $\Delta\sigma_r = \Delta\tau_{r\theta} = 0$ at $r = \infty$ (see Appendix A). Again, from Yuen (1979), the change in radial, tangential, and shear stress are

$$[8a] \quad \Delta\sigma_{Rg}^D = Q_o \left[3 \left(\frac{R_3}{r} \right)^4 - 4 \left(\frac{R_3}{r} \right)^2 \right] \cos 2\theta$$

$$[8b] \quad \Delta\sigma_{\theta g}^D = -3Q_o \left(\frac{R_3}{r} \right)^4 \cos 2\theta$$

and

$$[8c] \quad \Delta\tau_{R\theta g}^D = Q_o \left[3 \left(\frac{R_3}{r} \right)^4 - 2 \left(\frac{R_3}{r} \right)^2 \right] \sin 2\theta$$

and the radial and tangential displacements in the ground due to the tunnel excavation are, from Hooke’s Law,

$$[9a] \quad u_g^D = \int \varepsilon_r dr = \frac{Q_o(1 + \nu_g)}{E_g} \left[4(1 - \nu_g) \frac{R_3^2}{r} - \frac{R_3^4}{r^3} \right] \cos 2\theta$$

$$[9b] \quad v_g^D = \int \left[\varepsilon_\theta - \frac{u_g^D}{r} \right] r d\theta = -\frac{Q_o(1 + \nu_g)}{E_g} \left[2(1 - \nu_g) \frac{R_3^2}{r} + \frac{R_3^4}{r^3} \right] \sin 2\theta$$

Combined solution

The overall ground response due to full stress relief at $r = R_3$ can be obtained by superposition of the hydrostatic and deviatoric solutions presented above. For example, eqs. [4] and [9a] can be combined to obtain the radial displacement, u_g , in the ground viz.

$$[10a] \quad u_g = \frac{P_o(1 + \nu_g)R_3^2}{E_g r} + \frac{Q_o(1 + \nu_g)}{E_g} \left[4(1 - \nu_g) \frac{R_3^2}{r} - \frac{R_3^4}{r^3} \right] \cos 2\theta$$

Similarly, the tangential displacement, v_g , is

$$[10b] \quad v_g = -\frac{Q_o(1 + \nu_g)}{E_g} \left[2(1 - 2\nu_g) \frac{R_3^2}{r} + \frac{R_3^4}{r^3} \right] \sin 2\theta$$

and the radial, tangential, and shear stresses are

$$[11a] \quad \sigma_{Rg} = P_o \left[1 - \left(\frac{R_3}{r} \right)^2 \right] + Q_o \left[1 + 3 \left(\frac{R_3}{r} \right)^4 - 4 \left(\frac{R_3}{r} \right)^2 \right] \cos 2\theta$$

$$[11b] \quad \sigma_{\theta g} = P_o \left[1 + \left(\frac{R_3}{r} \right)^2 \right] - Q_o \left[1 + 3 \left(\frac{R_3}{r} \right)^4 \right] \cos 2\theta$$

and

$$[11c] \quad \tau_{R\theta g} = -Q_o \left[1 + 2 \left(\frac{R_3}{r} \right)^2 - 3 \left(\frac{R_3}{r} \right)^4 \right] \sin 2\theta$$

Stresses and displacements in the ground due to liner reactions

For the hydrostatic component, the liner reaction at $r = R_3$ in the radial direction is denoted by σ_{N2}^H (see Fig. 4). For the deviatoric component, the liner reaction at $r = R_3$ comprises both normal and tangential components denoted by $\sigma_{N2}^D \cos 2\theta$ and $\tau_{T2} \sin 2\theta$, respectively (see Fig. 5).

Hydrostatic component

The stresses and displacements at the interface between the ground and the outer lining due to the reactive force, σ_{N2}^H are from Yuen (1979)

$$[12a] \quad \sigma_{Rg \text{ react}}^H = \sigma_{N2}^H \left(\frac{R_3}{r} \right)^2$$

$$[12b] \quad \sigma_{\theta g \text{ react}}^H = -\sigma_{N2}^H \left(\frac{R_3}{r} \right)^2$$

$$[12c] \quad u_{Rg \text{ react}}^H(r = R_3) = -\frac{\sigma_{N2}^H (1 + \nu_g) R_3^2}{E_g r}$$

Deviatoric component, Q_o

For the boundary conditions, $\sigma_R = \sigma_{N2}^D \cos 2\theta$ and $\tau_{R\theta} = -\tau_{T2} \sin 2\theta$ at $r = R_3$ and $\tau_{R\theta} = \sigma_R = 0$ at $r = \infty$, the stresses and displacements in the ground medium due to the reactive forces, σ_{N2}^D and τ_{T2} are (Yuen 1979)

$$[13] \quad \sigma_{Rg \text{ react}}^D = \left[2(\sigma_{N2}^D + \tau_{T2}) \left(\frac{R_3}{r} \right)^2 - (\sigma_{N2}^D + 2\tau_{T2}) \left(\frac{R_3}{r} \right)^4 \right] \cos 2\theta$$

$$[14] \quad \sigma_{\theta g \text{ react}}^D = (2\tau_{T2} + \sigma_{N2}^D) \left(\frac{R_3}{r} \right)^4 \cos 2\theta$$

$$[15] \quad \tau_{R\theta g \text{ react}}^D = \left[(\sigma_{N2}^D + \tau_{T2}) \left(\frac{R_3}{r} \right)^2 - (\sigma_{N2}^D + 2\tau_{T2}) \left(\frac{R_3}{r} \right)^4 \right] \sin 2\theta$$

$$[16] \quad u_{g \text{ react}}^D = \frac{(1 + \nu_g) r}{3E_g} \left[(\sigma_{N2}^D + 2\tau_{T2}) \left(\frac{R_3}{r} \right)^4 - 6(1 - \nu_g)(\sigma_{N2}^D + \tau_{T2}) \left(\frac{R_3}{r} \right)^2 \right] \cos 2\theta$$

$$[17] \quad v_{g \text{ react}}^D = \frac{(1 + \nu_g) r}{3E_g} \left[(\sigma_{N2}^D + 2\tau_{T2}) \left(\frac{R_3}{r} \right)^4 + 3(1 - 2\nu_g)(\sigma_{N2}^D + \tau_{T2}) \left(\frac{R_3}{r} \right)^2 \right] \sin 2\theta$$

Accordingly, the radial and tangential displacements at the interface of the ground and the outer lining ($r = R_3$) due to the reactive forces, σ_{N2}^D and τ_{T2} are

$$[18a] \quad u_{g \text{ react}}^D(r = R_3) = -\frac{(1 + \nu_g) R_3}{3E_g} \times [(5 - 6\nu_g)\sigma_{N2}^D + (4 - 6\nu_g)\tau_{T2}] \cos 2\theta$$

$$[18b] \quad v_{g \text{ react}}^D(r = R_3) = \frac{(1 + \nu_g) R_3}{3E_g} \times [(4 - 6\nu_g)\sigma_{N2}^D + (5 - 6\nu_g)\tau_{T2}] \sin 2\theta$$

Figs. 4 and 5 show the reactions at the extrados and intrados of the outer liner.

Equations for stresses and displacements of the outer liner

For the hydrostatic component (see Fig. 4), the liner reactions at $r = R_3$ and $r = R_2$ are in the radial direction and denoted by σ_{N2}^H and σ_{N1}^H , respectively. For the deviatoric component (see Fig. 5), the liner reactions at $r = R_3$ comprise both normal and tangential components denoted by $\sigma_{N2}^D \cos 2\theta$ and $\tau_{T2} \sin 2\theta$, respectively. In addition, there are normal and tangential reactions between the inner liner (Liner 1) and the outer liner (Liner 2) at $r = R_2$ denoted by $\sigma_{N1}^D \cos 2\theta$ and $\tau_{T1} \sin 2\theta$, respectively. Both Yuen (1979) and Ogawa (1986) have developed solutions for the stresses and displacements in a thick walled cylinder subject to these external loads, which are presented in Appendix A. The equations utilized in this paper are summarized below.

Hydrostatic component

In a similar manner to that used for the ground, the resultant radial, tangential, and shear stresses in the outer lining for the boundary conditions, $\sigma_R = \sigma_{N2}^H$ at $r = R_3$ and $\sigma_R = \sigma_{N1}^H$ at $r = R_2$, are

$$[19a] \quad \sigma_{R_{L2}}^H = \sigma_{N1}^H \left[\frac{(R_2/r)^2 - h}{1 - h} \right] + \sigma_{N2}^H \left[\frac{1 - (R_2/r)^2}{1 - h} \right]$$

$$[19b] \quad \sigma_{\theta_{L2}}^H = -\sigma_{N1}^H \left[\frac{(R_2/r)^2 + h}{1 - h} \right] + \sigma_{N2}^H \left[\frac{1 + (R_2/r)^2}{1 - h} \right]$$

and

$$[19c] \quad \tau_{r\theta_{L2}}^H = 0$$

where $h = (R_2/R_3)^2$. The radial displacement of the outer lining, u_{L2}^H , is

$$[20] \quad u_{L2}^H = \int \varepsilon_{\theta 2}^H dr = \frac{(1 + \nu_2)r}{E_2(1 - h)} \left\{ \left[-\frac{R_2^2}{r^2}(1 - 2\nu_2)h \right] \sigma_{N1}^H + \left[\frac{R_2^2}{r^2} + (1 - 2\nu_2) \right] \sigma_{N2}^H \right\}$$

For $r = R_2$ and $r = R_3$, the radial displacements at the intrados and the extrados are

$$[21] \quad u_{L2}^H(r = R_3) = \frac{(1 + \nu_2)R_3}{E_2(1 - h)} \left\{ [-2(1 - \nu_2)h] \sigma_{N1}^H + (h + 1 - 2\nu_2) \sigma_{N2}^H \right\}$$

$$[22] \quad u_{L2}^H(r = R_2) = \frac{(1 + \nu_2)R_2}{E_2(1 - h)} \left\{ [-1 - (1 - 2\nu_2)h] \sigma_{N1}^H + [2(1 - \nu_2)] \sigma_{N2}^H \right\}$$

Deviatoric component

For the deviatoric component the radial and tangential displacements of the outer lining are

$$[23] \quad u_{L2}^D = \int \varepsilon_r dr = \frac{2(1 + \nu_2)r}{E_2} \times \left[-A - 2\nu_2 Br^2 + \frac{C}{r^4} + 2(1 - \nu_2) \frac{D}{r^2} \right] \cos 2\theta$$

and

$$[24] \quad v_{L2}^D = \int \left(\varepsilon_{\theta} - \frac{u_{2D}}{r} \right) r d\theta = \frac{2(1 + \nu_2)r}{E_2} \times \left[A + (3 - 2\nu_2) Br^2 + \frac{C}{r^4} - (1 - 2\nu_2) \frac{D}{r^2} \right] \sin 2\theta$$

Accordingly, the stresses and displacements at the interface between the ground and the outer lining (at $r = R_3$) due to the reactive force, σ_{N1}^D , σ_{N2}^D , τ_{T1} , and τ_{T2} are

$$[25a] \quad \sigma_{R_{L2}}^D(r = R_3) = -\left(2A + 6\frac{C}{R_3^4} + 4\frac{D}{R_3^2} \right) \cos 2\theta = \sigma_{N2}^D \cos 2\theta$$

$$[25b] \quad \sigma_{\theta_{L2}}^D(r = R_3) = \left(2A + 12BR_3^2 + 6\frac{C}{R_3^4} \right) \cos 2\theta$$

$$[25c] \quad \tau_{R\theta_{L2}}^D = \left(2A + 6BR_3^2 - 6\frac{C}{R_3^4} - 2\frac{D}{R_3^2} \right) \sin 2\theta = -\tau_{T2} \sin 2\theta$$

$$[26] \quad u_{L2}^D(r = R_3) = \frac{(1 + \nu_2)R_3}{3E_2(1 - h)^3} \times (\alpha_2 \sigma_{N2}^D + \beta_2 \tau_{T2} + \chi_2 \sigma_{N1}^D + \delta_2 \tau_{T1}) \cos 2\theta$$

and

$$[27] \quad v_{L2}^D(r = R_3) = \frac{(1 + \nu_2)R_3}{3E_2(1 - h)^3} \times (\psi_2 \sigma_{N2}^D + \gamma_2 \tau_{T2} + \eta_2 \sigma_{N1}^D + \omega_2 \tau_{T1}) \sin 2\theta$$

where the coefficients A, B, and C, and α_2 , β_2 , χ_2 , δ_2 , ψ_2 , γ_2 , λ_2 , and ω_2 are defined in Appendix A.

Similarly, at the intrados of the outer lining ($r = R_2$), the stresses and displacements are:

$$[28a] \quad \sigma_{R_{L2}}^D(r = R_2) = -\left(2A + 6\frac{C}{h^2 R_3^4} + 4\frac{D}{h R_3^2} \right) \cos 2\theta = \sigma_{N1}^D \cos 2\theta$$

$$[28b] \quad \sigma_{\theta_{L2}}^D(r = R_2) = \left(2A + 12BhR_3^2 + 6\frac{C}{h^2 R_3^4} \right) \cos 2\theta$$

$$[28c] \quad \tau_{R\theta_{L2}}^D(r = R_2) = \left(2A + 6BhR_3^2 - 6\frac{C}{h^2 R_3^4} - 2\frac{D}{h R_3^2} \right) \sin 2\theta = -\tau_{T1} \sin \theta$$

$$[29] \quad u_{L2}^D(r = R_2) = \frac{(1 + \nu_2)R_2}{3E_2(1 - h)^3} \times (\alpha_1 \sigma_{N2}^D + \beta_1 \tau_{T2} + \chi_1 \sigma_{N1}^D + \delta_1 \tau_{T1}) \cos 2\theta$$

and

$$[30] \quad v_{L2}^D(r = R_2) = \frac{(1 + \nu_2)R_2}{3E_2(1 - h)^3} \times (\psi_1 \sigma_{N2}^D + \gamma_1 \tau_{T2} + \eta_1 \sigma_{N1}^D + \omega_1 \tau_{T1}) \sin 2\theta$$

where α_1 , β_1 , χ_1 , δ_1 , ψ_1 , γ_1 , λ_1 , and ω_1 are defined in Appendix A.

Combined solution – hydrostatic and deviatoric

Now, the full solution for stresses and displacements in the outer liner (thick-walled cylinder) can be obtained by superposition of the hydrostatic and deviatoric solutions. Since the stresses and displacements at the intrados of the outer liner ($r = R_2$) are required to derive equations for the inner lining (Liner 1), the full solution at $r = R_2$ is as follows:

Fig. 4. Reaction stresses – hydrostatic component.

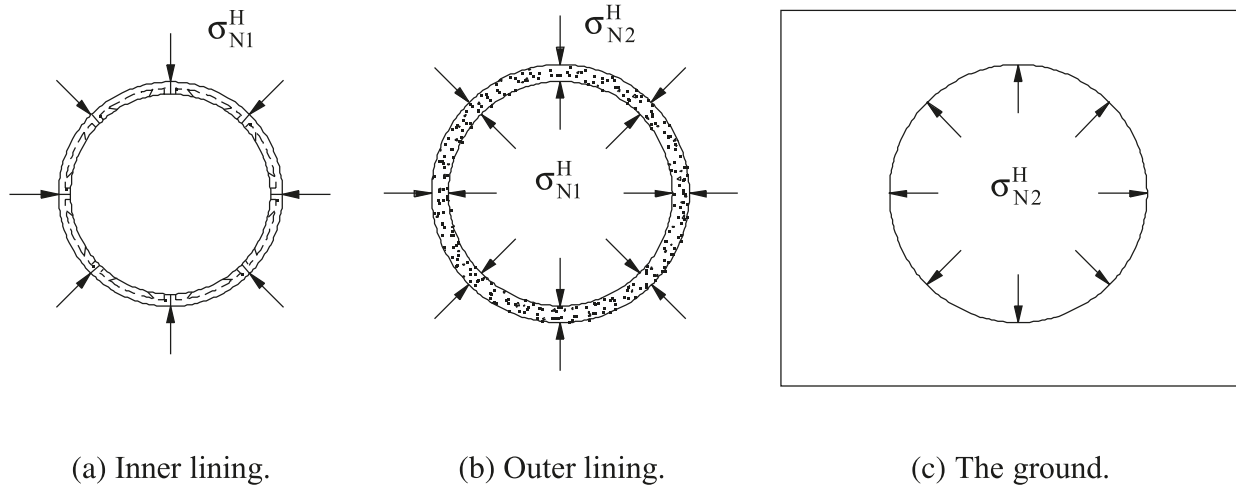
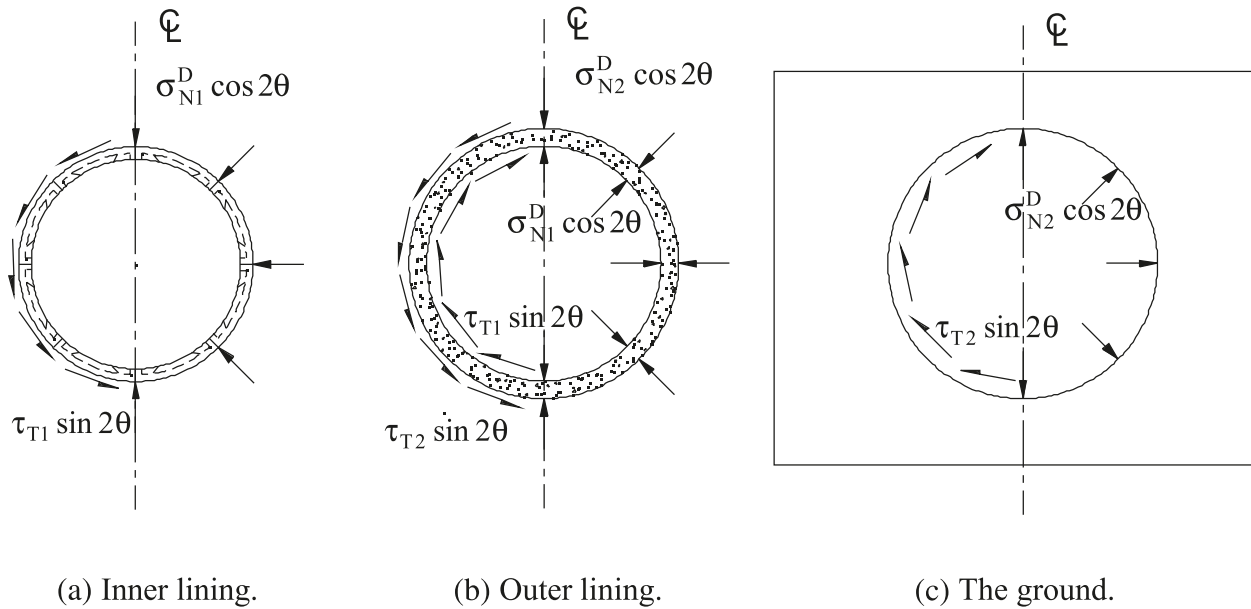


Fig. 5. Reaction stresses – deviatoric component.



$$[31a] \quad \sigma_{R_{L2}}(r = R_2) = \sigma_{N1}^H + \sigma_{N1}^D \cos 2\theta$$

$$[31b] \quad \sigma_{\theta_{L2}}(r = R_2) = \frac{-\sigma_{N1}^H(1+h) + 2\sigma_{N2}^H}{1-h} + \left(2A + 12BhR_3^2 + \frac{6C}{h^2R_3^4}\right) \cos 2\theta$$

$$[31c] \quad \tau_{R\theta_{L2}}(r = R_2) = -\tau_{T1} \sin 2\theta$$

$$[31d] \quad u_{L2}(r = R_2) = \frac{(1 + \nu_2)R_2}{E_2(1 - h)} \left\{ [-1 - (1 - 2\nu_2)h] \sigma_{N1}^H + [2(1 - \nu_2)] \sigma_{N2}^H \right\} + \frac{(1 + \nu_2)R_2}{3E_2(1 - h)^3} (\alpha_1 \sigma_{N2}^D + \beta_1 \tau_{T2} + \chi_1 \sigma_{N1}^D + \delta_1 \tau_{T1}) \cos 2\theta$$

and

$$[31e] \quad \nu_{L2}(r = R_2) = \frac{(1 + \nu_2)R_2}{3E_2(1 - h)^3} (\psi_1 \sigma_{N2}^D + \gamma_1 \tau_{T2} + \eta_1 \sigma_{N1}^D + \omega_1 \tau_{T1}) \sin 2\theta$$

Thus far, existing equations governing stresses and displacements in the ground outer liner have been presented. The following sections present the governing equations for the inner thin-walled shell and a new solution that accounts for ground–liner interaction in the case of a composite liner in elastic ground and accounting for some ground convergence prior to installation of the lining.

Equations for inner liner reactions

Governing equations

From Flügge (1966), the stresses and displacement of a thin shell are related by eqs. [32] and [33]

$$[32] \quad \frac{d^2v}{d\theta^2} + \frac{du}{d\theta} = -\frac{R^2}{D_c} \tau_{R\theta}$$

and

$$[33] \quad \frac{dv}{d\theta} + u + \frac{D_f}{D_c R^2} \left(\frac{d^4u}{d\theta^4} + 2 \frac{d^2u}{d\theta^2} + u \right) = \frac{R^2}{D_c} \sigma_R$$

where $D_c = E_1 A_1 / (1 - \nu_1^2)$, $D_f = E_1 I_1 / (1 - \nu_1^2)$, and A_1 , I_1 , E_1 , and ν_1 are the cross-sectional area, moment of inertia, elastic modulus, and Poisson’s ratio of the inner lining,

$$[35] \quad (-4C_8\psi_1 - 2C_8\alpha_1)\sigma_{N2}^D + (-4C_8\eta_1 - 2C_8\chi_1)\sigma_{N1}^D + (-4C_8\gamma_1 - 2C_8\beta_1)\tau_{T2} + \left(-4C_8\omega_1 - 2C_8\delta_1 - \frac{R_{c1}^2}{D_{c1}} \right) \tau_{T1} = 0$$

where $C_8 = (1 + \nu_2)R_2/[3E_2(1 - h)^3]$. Similarly, u , v , $\partial v/\partial\theta$, $\partial^2 u/\partial\theta^2$, and $\partial^4 u/\partial\theta^4$ can be obtained from eqs. [29], and [30] and substituted into eq. [33] with the boundary condition $\sigma_R = \sigma_{N1}^D \cos 2\theta$ to obtain

$$[36] \quad \left(2C_8\psi_1 + C_8\alpha_1 + \frac{9D_{F1}}{D_{c1}R_{c1}^2} C_8\alpha_1 \right) \sigma_{N2}^D + \left(2C_8\eta_1 + C_8\chi_1 + \frac{9D_{F1}}{D_{c1}R_{c1}^2} C_8\chi_1 - \frac{R_1^2}{D_{c1}} \right) \sigma_{N1}^D + \left(2C_8\gamma_1 + C_8\beta_1 + \frac{9D_{F1}}{D_{c1}R_{c1}^2} C_8\beta_1 \right) \tau_{T2} + \left(2C_8\omega_1 + C_8\delta_1 + \frac{9D_{F1}}{D_{c1}R_{c1}^2} C_8\delta_1 \right) \tau_{T1} = 0$$

For conditions of full slip at $r = R_2$, eq. [32] reduces to

$$[37a] \quad \frac{d^2v}{d\theta^2} + \frac{du}{d\theta} = 0$$

or

$$[37b] \quad u = -\frac{dv}{d\theta}$$

and, eq. [33] becomes

$$[38] \quad \frac{D_f}{D_c R^2} \left(\frac{d^4u}{d\theta^4} + 2 \frac{d^2u}{d\theta^2} + u \right) = \frac{R^2}{D_c} \sigma_R$$

Again, assuming $u_{L1}^D = u_{L2}^D$ at $r = R_2$ (continuity condition), partial derivatives $\partial^2 u/\partial\theta^2$ and $\partial^4 u/\partial\theta^4$ can be derived from eq. [30] and substituted into eq. [38] to obtain

$$[39] \quad \left(\frac{9D_{f1}}{R_{c1}^2} C_8\alpha_1 \right) \sigma_{N2}^D + \left(\frac{9D_{f1}}{R_{c1}^2} C_8\chi_1 - R_{c1}^2 \right) \sigma_{N1}^D = 0$$

So far equations have been developed relating the stresses and displacements in the ground, the outer liner, and the in-

ner liner. For the hydrostatic component of the solution, the radial reaction at $r = R_2$ is governed by eq. [34]. For the deviatoric component of the solution, eqs. [35] and [36] relate the reactions at $r = R_2$ to the elastic properties of the inner and outer linings and the ground for the case of no-slip. Equation [39] governs the case of full-slip. In the following sections, the principle of superposition is used to develop the full solution for a thick-walled cylinder and thin-walled shell in an infinite elastic medium.

Hydrostatic component

Since u and v do not vary with θ for the hydrostatic case, the following equation can be derived from eq. [33] for the radial displacement of the inner lining:

$$[34] \quad u_{L1}^H = \frac{R_{c1}^4}{D_{c1}R_{c1}^2 + D_{f1}} \sigma_{N1}^H$$

where σ_{N1}^H is the normal reaction at $r = R_2$ (see Fig. 4), and R_{c1} is the radius of the centroid of the inner lining.

Deviatoric component

For the deviatoric component, u and v vary with θ and two cases must be considered: full slip and no slip at $r = R_2$. Assuming the radial, u_{L1}^D , and tangential, v_{L1}^D , displacements of the inner lining are equal to the radial and tangential displacements of the outer lining at $r = R_2$ (no slip), then u , v , and partial derivatives $\partial^2 v/\partial\theta^2$, and $\partial u/\partial\theta$ can be derived from eqs. [29] and [30] and substituted into eq. [32] with the boundary condition $\tau_{R\theta} = \tau_{T1} \sin 2\theta$ to obtain

ner liner. For the hydrostatic component of the solution, the radial reaction at $r = R_2$ is governed by eq. [34]. For the deviatoric component of the solution, eqs. [35] and [36] relate the reactions at $r = R_2$ to the elastic properties of the inner and outer linings and the ground for the case of no-slip. Equation [39] governs the case of full-slip. In the following sections, the principle of superposition is used to develop the full solution for a thick-walled cylinder and thin-walled shell in an infinite elastic medium.

Interaction between the ground and composite liner system

Equations governing the interaction between the ground, the outer liner, and the inner liner can be derived by considering compatible displacements at each of the interfaces at $r = R_3$ and $r = R_2$. However, during construction of a shield driven tunnel, there is normally a gap between the extrados of the liner and the excavated diameter of the tunnel. Deformation of the ground into the gap prior to installation of the lining can lead to stress relief, which is ignored in current closed-form solutions. From eq. [10a], the tunnel conver-

gence, $\Delta D_F/D_0$, at springline corresponding to full stress relief is

$$[40] \quad \Delta D_F/D_0 = \frac{2P_0(1+\nu_g)R_3}{D_0E_g} + \frac{2Q_0(1+\nu_g)(3-4\nu_g)R_3}{D_0E_g}$$

Equation [41] is used to define the case where the springline convergence is less than that for full stress relief

$$[41] \quad \Delta D_P/D_0 = \frac{2\Omega P_0(1+\nu_g)R_3}{D_0E_g} + \frac{2\Omega Q_0(1+\nu_g)(3-4\nu_g)R_3}{D_0E_g}$$

where the parameter Ω denotes the fraction of the full stress relief solution caused by partial convergence of the tunnel before installation of the lining. The radial displacement into the gap is thus

$$[42a] \quad u_{\text{gap}} = \frac{\Omega P_0(1+\nu_g)R_3}{E_g} + \frac{\Omega Q_0(1+\nu_g)(3-4\nu_g)R_3}{E_g} \cos 2\theta$$

and the corresponding tangential displacement is

$$[42b] \quad v_{\text{gap}} = -\frac{\Omega Q_0(1+\nu_g)(1-2\nu_g)R_3}{E_g} \sin 2\theta$$

Provided that $\Delta D_P/D_0$ is less than the physical gap, eqs. [42a] and [42b] can be used to approximately account for some stress relief caused by ground convergence prior to installation of the liner as shown below. In the following section, full solutions are developed for a composite tunnel liner in an infinite elastic medium. The solutions are separated into hydrostatic and deviatoric components. As a result, the radial stress at $r = R_3$ takes the following general form:

$$[43a] \quad \sigma_R(r = R_3) = \sigma_{N_2}^H + \sigma_{N_2}^D \cos 2\theta$$

and the tangential reactions at $r = R_3$ are

$$[43b] \quad \tau_{R\theta}(r = R_3) = \tau_{T_2} \sin 2\theta$$

Similarly at $r = R_2$

$$[44a] \quad \sigma_R(r = R_2) = \sigma_{N_1}^H + \sigma_{N_1}^D \cos 2\theta$$

and

$$[44b] \quad \tau_{R\theta}(r = R_2) = \tau_{T_1} \sin 2\theta$$

Hydrostatic component

At the interface between the ground and the outer lining, the displacement of the outer lining, $u_{L_2}^H$, plus the radial displacement into the gap, u_{gap}^H , must equal the displacement of the ground caused by full stress relief, u_g^H , plus the displacement of the ground due to the reactive force, $\sigma_{N_2}^H$. Thus, the compatibility constrain at $r = R_3$ is

$$[45] \quad u_{L_2}^H(r = R_3) + u_{\text{gap}}^H = u_g^H(r = R_3) + u_{\text{react}}^H(r = R_3)$$

Substituting from eqs. [4], [12c], [21], and [42a] into eq. [45] gives

$$[46] \quad \frac{(1+\nu_2)R_3}{E_2(1-h)} \{[-2(1-\nu_2)h]\sigma_{N_1}^H + (h+1-2\nu_2)\sigma_{N_2}^H\} + \frac{\Omega P_0(1+\nu_g)R_3}{E_g} = \frac{P_0(1+\nu_g)R_3}{E_g} - \frac{\sigma_{N_2}^H(1+\nu_g)R_3}{E_g}$$

which can be simplified to

$$[47] \quad (1-\Omega)P_0 - \sigma_{N_2}^H = C_1(C_2\sigma_{N_1}^H + C_3\sigma_{N_2}^H)$$

where C_1 , C_2 , and C_3 are

$$C_1 = \frac{E_g(1+\nu_2)}{E_2(1+\nu_g)}$$

$$C_2 = -\frac{2(1-\nu_2)h}{(1-h)}$$

$$C_3 = \frac{h+(1-2\nu_2)}{(1-h)}$$

At the interface between the outer lining and the inner lining, the compatibility condition is

$$[48] \quad u_{L_2}^H(r = R_2) = u_{L_1}^H(r = R_2)$$

which implies that the radial displacement of the inner lining is equal to the radial displacement of the outer lining at $r = R_3$. Substituting eqs. [22] and [34] into eq. [48] and rearranging gives

$$[49] \quad C_4\sigma_{N_1}^H = C_5\sigma_{N_1}^H + C_6\sigma_{N_2}^H$$

where C_4 , C_5 , and C_6 are

$$C_4 = \frac{R_{c1}^4}{D_{c1}R_{c1}^2 + D_{f1}}$$

$$C_5 = \frac{(1+\nu_2)}{E_2(1-h)} [-1 - (1-2\nu_2)h]R_2$$

$$C_6 = \frac{2(1+\nu_2)(1-\nu_2)}{E_2(1-h)}R_2$$

The reactions $\sigma_{N_1}^H$ and $\sigma_{N_2}^H$ at $r = R_2$ and $r = R_3$, respectively, can be obtained by solving eqs. [47] and [49] to obtain

$$[50] \quad \sigma_{N_1}^H = \frac{(1-\Omega)P_0}{C_1(C_2 + C_3C_7) + C_7}$$

$$[51] \quad \sigma_{N_2}^H = \frac{(1-\Omega)P_0C_7}{C_1(C_2 + C_3C_7) + C_7}$$

where,

$$C_7 = \frac{(C_4 - C_5)}{C_6}$$

The above solution applies to conditions of slip and no slip at either of the interfaces at $r = R_2$ or $r = R_3$.

Deviatoric component – no slip at $r = R_2$ and $r = R_3$

Equation [45] can also be applied to the radial displacements resulting from the deviatoric component of the initial stress field. Thus, at $r = R_3$ the compatibility condition is

$$[52] \quad u_{L2}^D(r = R_3) + u_{gap}^D = u_g^D(r = R_3) + u_{g\ react}^D(r = R_3)$$

where $u_{L2}^D(r = R_3)$ is the radial displacement of the outer liner at $r = R_3$, u_{gap}^D is the radial displacement of the ground into the gap prior to installation of the liner, $u_g^D(r = R_3)$ is the ground displacement caused by full stress relief, and $u_{g\ react}^D(r = R_3)$ is the ground displacement due to the liner reaction. Substituting eqs. [26], [42a], [9a], and [18a] into eq. [52] gives

$$[53] \quad 3(1 - \Omega)Q_0(3 - 4\nu_g) = (C_{10} + C_9\alpha_2)\sigma_{N2}^D + (C_9\chi_2)\sigma_{N1}^D + (C_{11} + C_9\beta_2)\tau_{T2} + (C_9\delta_2)\tau_{T1}$$

where,

$$[56] \quad \begin{Bmatrix} \sigma_{N2}^D \\ \sigma_{N1}^D \\ \tau_{T2} \\ \tau_{T1} \end{Bmatrix} \times \begin{bmatrix} a_{11} & a_{12} & a_{13} & a_{14} \\ a_{21} & a_{22} & a_{23} & a_{24} \\ a_{31} & a_{32} & a_{33} & a_{34} \\ a_{41} & a_{42} & a_{43} & a_{44} \end{bmatrix} = \begin{Bmatrix} 0 \\ 0 \\ 3(1 - \Omega)Q_0(3 - 4\nu_g) \\ 3(1 - \Omega)Q_0(3 - 4\nu_g) \end{Bmatrix}$$

where,

$$a_{11} = -4C_8\psi_1 - 2C_8\alpha_1$$

$$a_{12} = -4C_8\eta_1 - 2C_8\chi_1$$

$$a_{13} = -4C_8\gamma_1 - 2C_8\beta_1$$

$$a_{14} = -4C_8\omega_1 - 2C_8\delta_1 - \frac{R_{c1}^2}{D_{C1}}$$

$$a_{21} = 2C_8\psi_1 + C_8\alpha_1 + \frac{9D_{F1}}{D_{C1}R_{c1}^2}C_8\alpha_1$$

$$a_{22} = 2C_8\eta_1 + C_8\chi_1 + \frac{9D_{F1}}{D_{C1}R_{c1}^2}C_8\chi_1 - \frac{R_{c1}^2}{D_{C1}}$$

$$a_{23} = 2C_8\gamma_1 + C_8\beta_1 + \frac{9D_{F1}}{D_{C1}R_{c1}^2}C_8\beta_1$$

$$C_9 = \frac{(1 + \nu_2)E_g}{(1 + \nu_g)E_2(1 - h)^3}$$

$$C_{10} = 5 - 6\nu_g$$

$$C_{11} = 4 - 6\nu_g$$

Similarly, the following compatibility equation can be derived for the tangential displacements:

$$[54] \quad v_{L2}^D(r = R_3) + v_{gap}^D = v_g^D(r = R_3) + v_{g\ react}^D(r = R_3)$$

Substituting eqs. [27], [42b], [9b], and [18b] into eq. [54] gives

$$[55] \quad 3(1 - \Omega)Q_0(3 - 4\nu_g) = (C_{11} - C_9\psi_2)\sigma_{N2}^D - (C_9\eta_2)\sigma_{N1}^D + (C_{10} - C_9\gamma_2)\tau_{T2} - (C_9\omega_2)\tau_{T1}$$

where C_9 , C_{10} , and C_{11} are defined above.

There are now four equations relating σ_{N1}^D , σ_{N2}^D , τ_{T1} , and τ_{T2} to Q_0 for the deviatoric component of the solution. Combining eqs. [35] and [36] for the inner lining and eqs. [53] and [55] for the outer lining gives the following system of equations:

$$a_{24} = 2C_8\omega_1 + C_8\delta_1 + \frac{9D_{F1}}{D_{C1}R_{c1}^2}C_8\delta_1$$

$$a_{31} = C_{10} + C_9\alpha_2$$

$$a_{32} = C_9\chi_2$$

$$a_{33} = C_{11} + C_9\beta_2$$

$$a_{34} = C_9\delta_2$$

$$a_{41} = C_{11} - C_9\psi_2$$

$$a_{42} = -C_9\eta_2$$

$$a_{43} = C_{10} - C_9\gamma_2$$

$$a_{44} = -C_9\omega_2$$

(Note: $C_8 = (1 + \nu_2)R_2/[3E_2(1 - h)^3]$)

Explicit solutions for $\sigma_{N1}^D, \sigma_{N2}^D, \tau_{T1}$, and τ_{T2} are

$$[57] \quad \sigma_{N2}^D = \frac{3(1 - \Omega)Q_0(3 - 4\nu_g)\left(\frac{a_{13}}{\Lambda} + a_{14}\right)}{(a_{31} + a_{32}\Gamma)\left(\frac{a_{13}}{\Lambda} + a_{14}\right) - (a_{11} + a_{12}\Gamma)\left(\frac{a_{33}}{\Lambda} + a_{34}\right)}$$

$$[58] \quad \sigma_{N1}^D = \Gamma\sigma_{N2}^D$$

$$[59] \quad \tau_{T2} = -\frac{3(1 - \Omega)Q_0(3 - 4\nu_g)(a_{11} + a_{12}\Gamma)}{(a_{31} + a_{32}\Gamma)(a_{13} + a_{14}\Lambda) - (a_{11} + a_{12}\Gamma)(a_{33} + a_{34}\Lambda)}$$

and

$$[60] \quad \tau_{T1} = \Lambda\tau_{T2}$$

where,

$$\Gamma = -\frac{(a_{31} - a_{41})(a_{14}a_{23} - a_{24}a_{13}) + (a_{33} - a_{43})(a_{11}a_{24} - a_{21}a_{14}) + (a_{34} - a_{44})(a_{21}a_{13} - a_{11}a_{23})}{(a_{32} - a_{42})(a_{14}a_{23} - a_{24}a_{13}) + (a_{33} - a_{43})(a_{12}a_{24} - a_{22}a_{14}) + (a_{34} - a_{44})(a_{22}a_{13} - a_{12}a_{23})}$$

and

$$\Lambda = -\frac{(a_{31} - a_{41})(a_{22}a_{13} - a_{12}a_{23}) + (a_{32} - a_{42})(a_{11}a_{23} - a_{21}a_{13}) + (a_{33} - a_{43})(a_{21}a_{12} - a_{11}a_{22})}{(a_{31} - a_{41})(a_{22}a_{14} - a_{12}a_{24}) + (a_{32} - a_{42})(a_{11}a_{24} - a_{21}a_{14}) + (a_{34} - a_{44})(a_{21}a_{12} - a_{11}a_{22})}$$

Deviatoric component – full slip at $r = R_2$ and $r = R_3$

For the case of full slip at $r = R_2$ and $r = R_3$, the boundary conditions are: $\sigma_R = \sigma_{N2}^D \cos 2\theta$ and $\tau_{R\theta} = 0$ at $r = R_3$, $\sigma_R = \sigma_{N1}^D \cos 2\theta$ and $\tau_{R\theta} = 0$ at $r = R_2$, and $\sigma_R = \tau_{R\theta} = 0$ at $r = \infty$. Thus, from eq. [18a] the radial displacement in the ground at $r = R_3$ is

$$[61] \quad u_{g,react}^D(r = R_3) = -\frac{(1 + \nu_g)R_3}{3E_g} [(5 - 6\nu_g)\sigma_{N2}^D] \cos 2\theta$$

Also from eq. [26], the radial displacement of the outer lining at $r = R_3$ is

$$[62] \quad u_{L2}^D(r = R_3) = \frac{(1 + \nu_2)R_3}{3E_2(1 - h)^3} (\alpha_2\sigma_{N2}^D + \chi_2\sigma_{N1}^D) \cos 2\theta$$

Considering compatibility of the radial displacement at $r = R_3$ (see eq. [52]), the following equation can be developed by combining eqs. [62], [42a], [9a], and [61]:

$$[63] \quad \frac{(1 + \nu_2)R_3}{3E_2(1 - h)^3} (\alpha_2\sigma_{N2}^D + \chi_2\sigma_{N1}^D) \cos 2\theta + \frac{\Omega Q_0(1 + \nu_g)(3 - 4\nu_g)R_3}{E_g} \cos 2\theta = \frac{Q_0(1 + \nu_g)(3 - 4\nu_g)R_3}{E_g} \cos 2\theta - \frac{(1 + \nu_g)R_3}{3E_g} [(5 - 6\nu_g)\sigma_{N2}^D] \cos 2\theta$$

which can be rearranged to give

$$[64] \quad 3(1 - \Omega)Q_0(3 - 4\nu_g) = (C_{10} + C_9\alpha_2)\sigma_{N2}^D + (C_9\chi_2)\sigma_{N1}^D$$

Thus, for full slip at $r = R_2$ and $r = R_3$, there are now two equations relating σ_{N1}^D and σ_{N2}^D to Q_0 for the deviatoric component. Hence, by solving eqs. [39] and [64], the reactions σ_{N1}^D and σ_{N2}^D at $r = R_2$ and $r = R_3$ are

$$[65] \quad \sigma_{N1}^D = C_{12}3(1 - \Omega)Q_0(3 - 4\nu_g) \left(-\frac{9D_{f1}}{R_{c1}^2} C_8\alpha_1 \right)$$

$$[66] \quad \sigma_{N2}^D = C_{12}3(1 - \Omega)Q_0(3 - 4\nu_g) \left(\frac{9D_{f1}}{R_{c1}^2} C_8\chi_1 - R_{c1}^2 \right)$$

where,

$$C_{12} = \frac{1}{(C_{10} + C_9\alpha_2) \left(\frac{9D_{f1}}{R_{c1}^2} C_8\chi_1 - R_{c1}^2 \right) - (C_9\chi_2) \left(\frac{9D_{f1}}{R_{c1}^2} C_8\alpha_1 \right)}$$

Deviatoric component – full slip at R_2 , no slip at R_3

For the case of full slip at $r = R_2$ and no slip at $r = R_3$ the boundary conditions are: $\sigma_R = \sigma_{N2}^D \cos 2\theta$ and $\tau_{R\theta} = \tau_{T2} \sin 2\theta$ at $r = R_3$, $\sigma_R = \sigma_{N1}^D \cos 2\theta$ and $\tau_{R\theta} = 0$ at $r = R_2$, and $\sigma_R = \tau_{R\theta} = 0$ at $r = \infty$. Using a similar approach to that followed for the previous two cases, the following system of equations can be developed:

$$[67] \quad \begin{Bmatrix} \sigma_{N2}^D \\ \sigma_{N1}^D \\ \tau_{T2} \end{Bmatrix} \times \begin{bmatrix} b_{11} & b_{12} & b_{13} \\ b_{21} & b_{22} & b_{23} \\ b_{31} & b_{32} & b_{33} \end{bmatrix} = \begin{Bmatrix} 3(1-\Omega)Q_0(3-4\nu_g) \\ 3(1-\Omega)Q_0(3-4\nu_g) \\ 0 \end{Bmatrix}$$

where,

$$b_{11} = C_{10} + C_9\alpha_2$$

$$b_{12} = C_9\chi_2$$

$$b_{13} = C_{11} + C_9\beta_2$$

$$b_{21} = C_{11} - C_9\psi_2$$

$$b_{22} = -C_9\eta_2$$

$$b_{23} = C_{10} - C_9\gamma_2$$

$$b_{31} = \frac{9D_{f1}}{R_{c1}^2} C_8\alpha_1$$

$$b_{32} = \frac{9D_{f1}}{R_{c1}^2} C_8\chi_1 - R_{c1}^2$$

$$b_{33} = \frac{9D_{f1}}{R_{c1}^2} C_8\beta_1$$

The solution to eq. [67] is

$$[68] \quad \sigma_{N2}^D = \frac{3(1-\Omega)Q_0(3-4\nu_g)}{b_{11} + b_{12}\Gamma - b_{13}(b_{31} + b_{32}\Gamma)/b_{33}}$$

$$[69] \quad \sigma_{N1}^D = \Gamma\sigma_{N2}^D$$

$$[70] \quad \tau_{T2} = -\frac{b_{31} + b_{32}\Gamma}{b_{33}}\sigma_{N2}^D$$

where,

$$\Gamma = \frac{b_{31}(b_{23} - b_{13}) + b_{33}(b_{11} - b_{21})}{b_{33}(b_{22} - b_{12}) + b_{32}(b_{13} - b_{23})}$$

Deviatoric component – no slip at R_2 , full slip at R_3

For the case of no slip at $r = R_2$ and full slip at $r = R_3$ the boundary conditions are: $\sigma_R = \sigma_{N2}^D \cos 2\theta$ and $\tau_{R\theta} = 0$ at $r = R_3$, $\sigma_R = \sigma_{N1}^D \cos 2\theta$ and $\tau_{R\theta} = \tau_{T1} \sin 2\theta$ at $r = R_2$, and $\sigma_R = \tau_{T\theta} = 0$ at $r = \infty$. Similar to the previous cases, the following system of equations can be developed:

$$[71] \quad \begin{Bmatrix} \sigma_{N2}^D \\ \sigma_{N1}^D \\ \tau_{T1} \end{Bmatrix} \times \begin{bmatrix} c_{11} & c_{12} & c_{13} \\ c_{21} & c_{22} & c_{23} \\ c_{31} & c_{32} & c_{33} \end{bmatrix} = \begin{Bmatrix} 3(1-\Omega)Q_0(3-4\nu_g) \\ 0 \\ 0 \end{Bmatrix}$$

where,

$$c_{11} = C_{10} + C_9\alpha_2$$

$$c_{12} = C_9\chi_2$$

$$c_{13} = C_9\delta_2$$

$$c_{21} = 2C_8\psi_1 + C_8\alpha_1 + \frac{9D_{f1}}{D_{C1}R_{c1}^2} C_8\alpha_1$$

$$c_{22} = 2C_8\eta_1 + C_8\chi_1 + \frac{9D_{f1}}{D_{C1}R_{c1}^2} C_8\chi_1 - \frac{R_{c1}^2}{D_{C1}}$$

$$c_{23} = 2C_8\omega_1 + C_8\delta_1 + \frac{9D_{f1}}{D_{C1}R_{c1}^2} C_8\delta_1$$

$$c_{31} = -4C_8\psi_1 - 2C_8\alpha_1$$

$$c_{32} = -4C_8\eta_1 - 2C_8\chi_1$$

$$c_{33} = -4C_8\omega_1 - 2C_8\delta_1 - \frac{R_{c1}^2}{D_{C1}}$$

Explicit solutions for the unknowns σ_{N1}^D , σ_{N2}^D , and τ_{T1} are

$$[72] \quad \sigma_{N2}^D = \frac{3(1-\Omega)Q_0(3-4\nu_g)}{c_{11} + c_{12}\Gamma - c_{13}(c_{31} + c_{32}\Gamma)/c_{33}}$$

$$[73] \quad \sigma_{N1}^D = \Gamma\sigma_{N2}^D$$

$$[74] \quad \tau_{T1} = -\frac{c_{31} + c_{32}\Gamma}{c_{33}}\sigma_{N2}^D$$

where,

$$\Gamma = \frac{c_{23}c_{31} - c_{21}c_{33}}{c_{22}c_{33} - c_{23}c_{32}}$$

Moment and thrust – inner liner

From Flügge (1966) the moments and thrusts for a thin-walled shell in polar coordinates are

$$[75a] \quad M = -\frac{D_f}{R^2} \left(u + \frac{d^2 u}{d\theta^2} \right)$$

$$[75b] \quad T = \frac{D_c}{R} \left(u + \frac{dv}{d\theta} \right) + \frac{M}{R}$$

Hydrostatic component

From eqs. [75a] and [75b], moments and thrusts in the inner lining due to the hydrostatic component of the solution are

$$[76a] \quad M^H = -\frac{D_{f1} R_{c1}^2}{D_{c1} R_{c1}^2 + D_{f1}} \sigma_{N1}^H$$

$$[76b] \quad T^H = \frac{D_{c1} R_{c1}^3}{D_{c1} R_{c1}^2 + D_{f1}} \sigma_{N1}^H + \frac{M^H}{R_{c1}}$$

Equations [76a] and [76b] apply to both cases of slip and no slip at $r = R_2$.

Deviatoric component – no slip at $r = R_2$ and $r = R_3$

Using eqs. [75a] and [75b], moments and thrusts in the inner lining due to the deviatoric component are:

$$[77a] \quad M^D = -\frac{D_{f1}}{R_{c1}^2} [-3C_8(\alpha_1 \sigma_{N2}^D + \beta_1 \tau_{T2} + \chi_1 \sigma_{N1}^D + \delta_1 \tau_{T1})] \cos 2\theta$$

and

$$[77b] \quad T^D = \left\{ \frac{D_{c1}}{R_{c1}} C_8 [(\alpha_1 + 2\psi_1) \sigma_{N2}^D + (\beta_1 + 2\gamma_1) \tau_{T2} + (\chi_1 + 2\eta_1) \sigma_{N1}^D + (\delta_1 + 2\omega_1) \tau_{T1}] + \frac{M^D}{R_{c1}} \right\} \cos 2\theta$$

Deviatoric component – full slip $r = R_2$ and $r = R_3$

For conditions of full slip at $r = R_2$, from eq. [37], u equals $-dv/d\theta$ and hence, eq. [75b] simplifies to

$$[78] \quad T = \frac{M}{R}$$

giving,

$$[79a] \quad M^D = -\frac{D_{f1}}{R_{c1}^2} [-3C_8(\alpha_1 \sigma_{N2}^D + \chi_1 \sigma_{N1}^D)] \cos 2\theta$$

$$[79b] \quad T^D = \frac{M^D}{R_{c1}} \cos 2\theta$$

Using a similar process, moment and thrust for other cases are given by eqs. [80] and [81].

Deviatoric component – full slip at R_2 , no slip at R_3

$$[80a] \quad M^D = -\frac{D_{f1}}{R_{c1}^2} [-3C_8(\alpha_1 \sigma_{N2}^D + \chi_1 \sigma_{N1}^D + \beta_1 \tau_{T2})] \cos 2\theta$$

$$[80b] \quad T^D = \frac{M^D}{R_{c1}} \cos 2\theta$$

Deviatoric component – no slip at R_2 , full slip at R_3

$$[81a] \quad M^D = -\frac{D_{f1}}{R_{c1}^2} [-3C_8(\alpha_1 \sigma_{N2}^D + \chi_1 \sigma_{N1}^D + \delta_1 \tau_{T1})] \cos 2\theta$$

$$[81b] \quad T^D = \left\{ \frac{D_{c1}}{R_{c1}} C_8 [(\alpha_1 + 2\psi_1) \sigma_{N2}^D + (\chi_1 + 2\eta_1) \sigma_{N1}^D + (\delta_1 + 2\omega_1) \tau_{T1}] + \frac{M^D}{R_{c1}} \right\} \cos 2\theta$$

Thus, full solutions for displacement, moment, and thrust in the inner thin-walled shell have been derived and presented. In the following sections, the solution is applied to a composite lining in an infinite elastic medium.

Typical results

To illustrate some of the characteristics of the solution, normalized displacements, thrusts, and moments are presented in this section versus the flexibility ratio defined in accordance with Einstein and Schwartz (1979) viz.

$$[82a] \quad F = \frac{E_g R_{c1}^3 (1 - \nu_g^2)}{E_1 I_1 (1 - \nu_g^2)}$$

and the normalized displacements, u_c , thrust, T_c , and moment, M_c , are

$$[82b] \quad u_c = \frac{u_{L1} E_g}{\sigma_v R_{c1} (1 + \nu_g)}$$

$$[82c] \quad T_c = \frac{T}{\sigma_v R_{c1}}$$

and

$$[82d] \quad M_c = \frac{M}{\sigma_v R_{c1}^2}$$

The effect of ground convergence prior to liner installation

Figures 6 through 9 show the effect of Ω on displacements, moment, and thrust in the inner lining. For this group of figures, the thickness of the outer liner was assumed to be 0.001 m. Consequently, the outer lining has no effect on the inner lining behaviour, and for $\Omega = 0$ the composite lining solution is essentially equivalent to the Einstein and Schwartz (1979) solution. In accordance with eqs. [40] and [41], the parameter Ω represents the fraction of the full

Fig. 6. Normalized radial displacement at the crown of the inner lining.

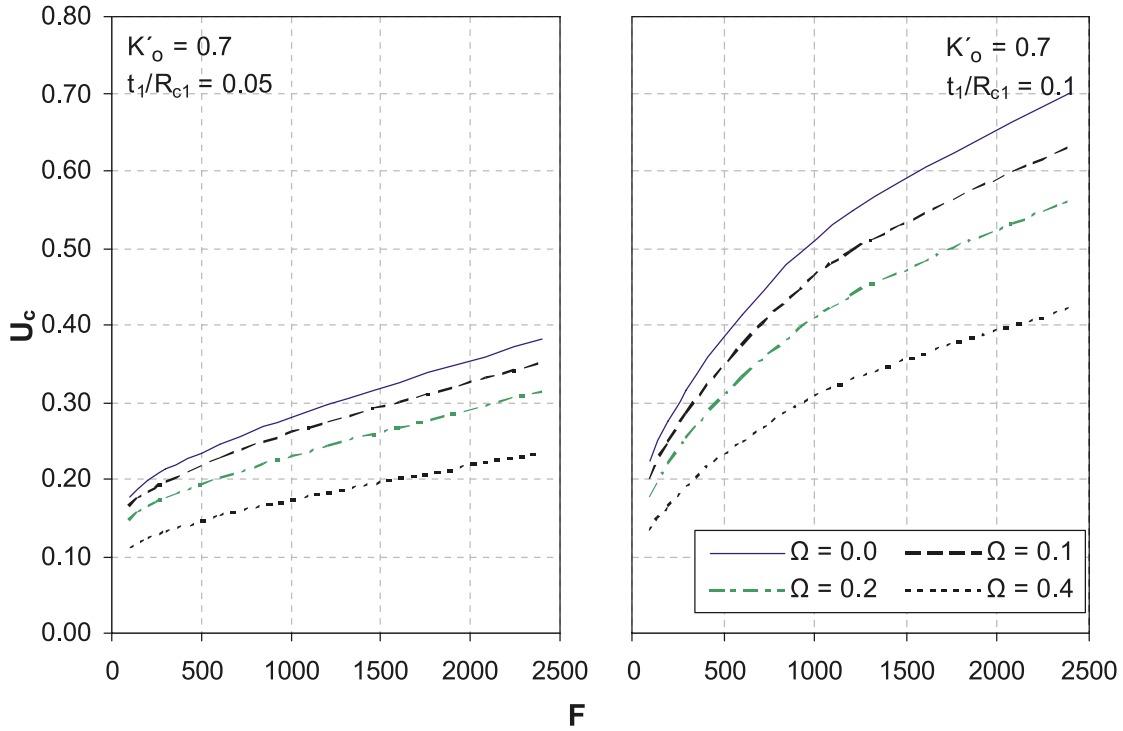


Fig. 7. Normalized radial displacement at the springline of the inner lining.

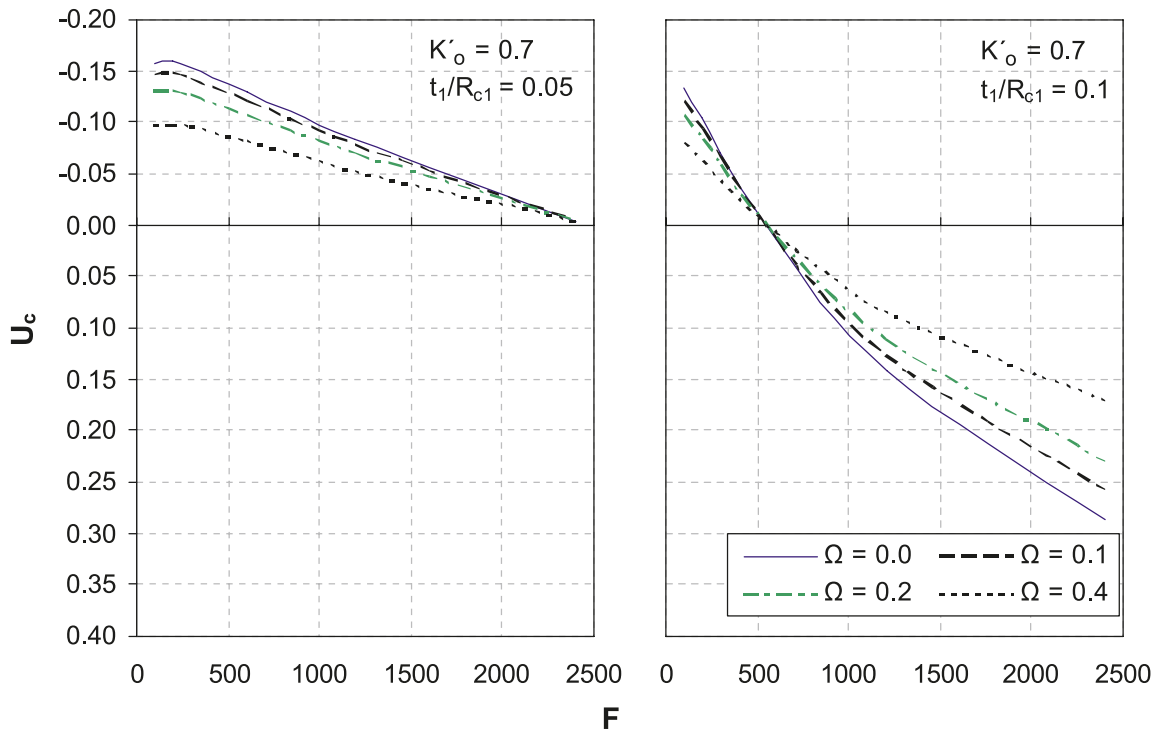


Fig. 8. Normalized thrust at the springline of the inner lining.

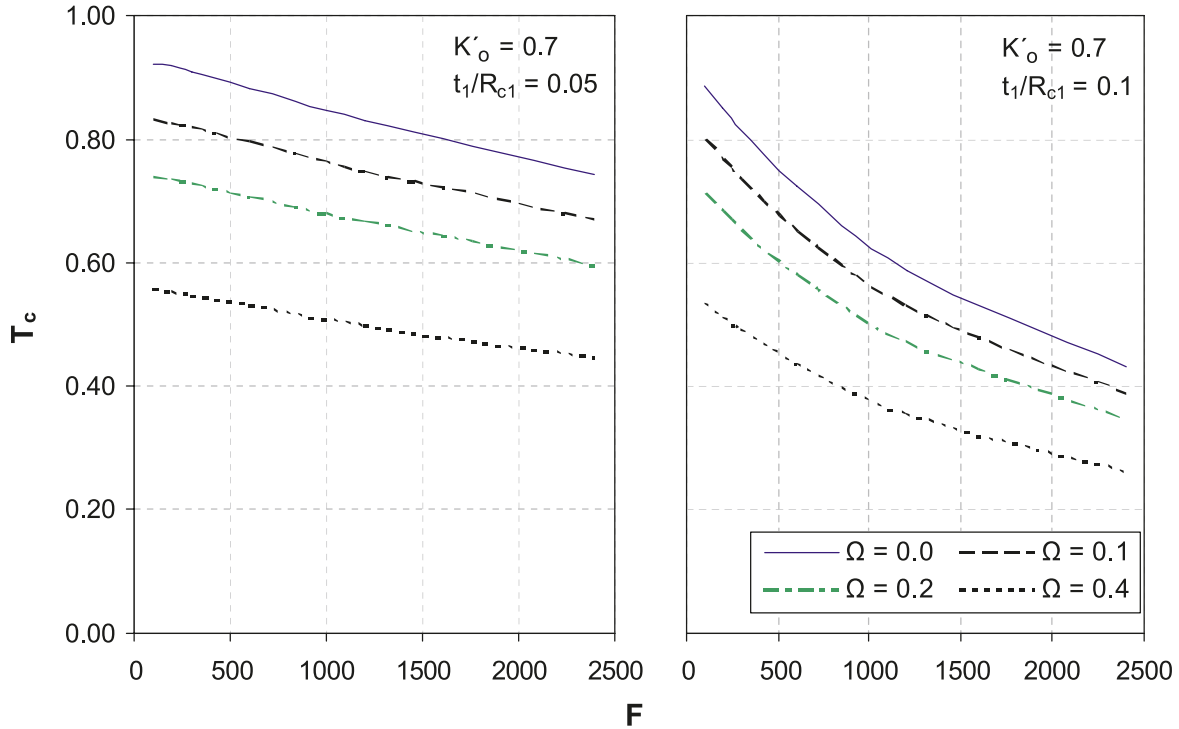
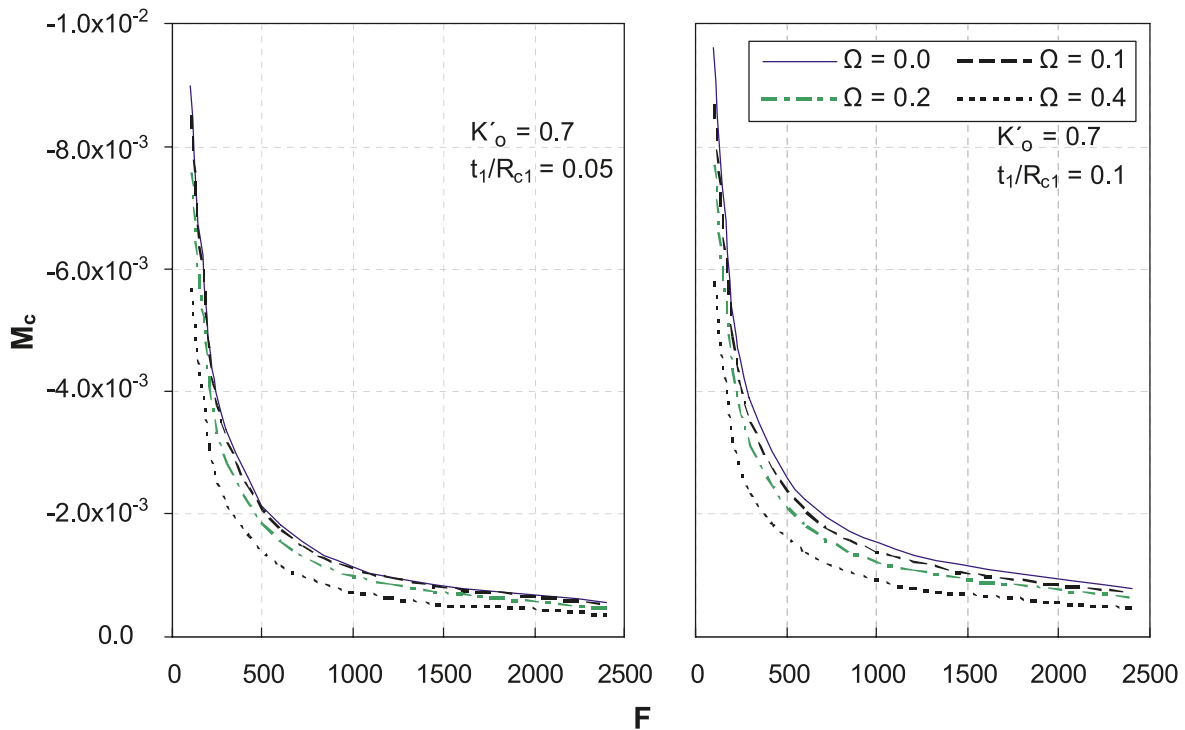


Fig. 9. Moment at the springline of the inner lining.



stress relief solution (eqs. [10a] and [10b]) that is permitted to occur prior to installation of the lining. As shown in each of the figures, solutions have been developed for $K'_o = 0.7$ and thickness ratios, t_1/R_{c1} of 0.05 and 0.1 for the inner lining.

It can be seen from Fig. 6 that the radial displacement at the crown of the inner lining increases as the flexibility ratio

increases. For $\Omega = 0$, the composite lining solution reduces to a single lining solution that agrees with Einstein and Schwartz (1979). Furthermore, the radial displacement of the inner lining at the crown decreases as the degree of ground convergence prior to the liner installation increases (e.g., as Ω increases). Similar trends in behaviour can also be observed in Fig. 7 for the springline. At the springline,

Fig. 10. Radial displacement at the crown and the springline of the inner lining.

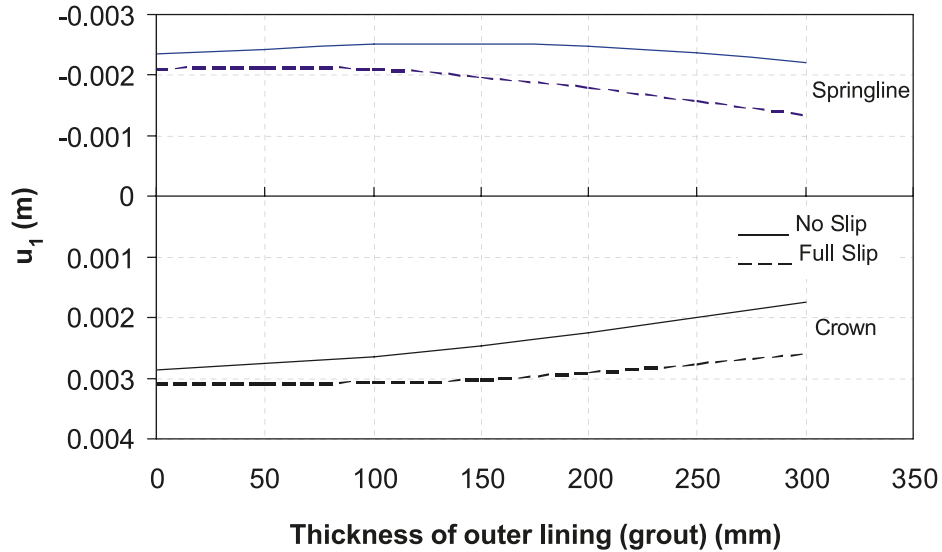


Fig. 11. Thrust at the crown and the springline of the inner lining.

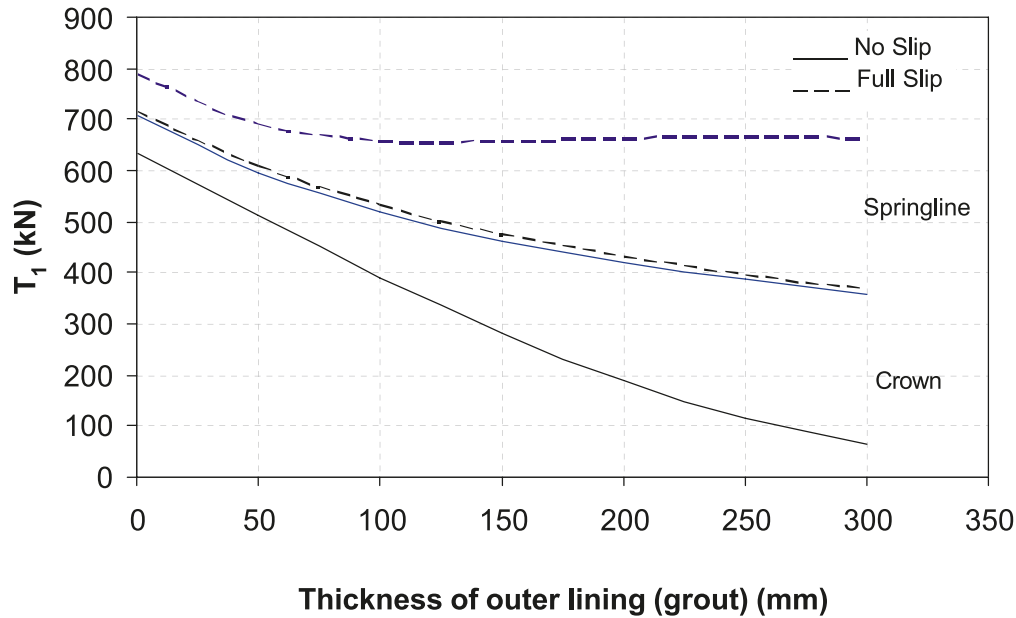


Table 2. Material parameters used in the study.

Parameter	Value
Soil elastic modulus, E_g (MPa)	90
Soil Poisson's ratio, ν_g	0.4
Coefficient of earth pressure at rest, K'_o	0.7
Initial vertical stress, σ_v (kN/m ²)	344
Initial horizontal stress, σ_h (kN/m ²)	241
Elastic modulus of concrete, E_1 (GPa)	30
Poisson's ratio of concrete, ν_1	0.2
Elastic modulus of grout, E_2 (GPa)	20
Poisson's ratio of grout, ν_2	0.2

however, the radial displacement of the inner lining is generally inward for low flexibility ratios. For thickness ratios, t_1/R_{c1} , of 0.05 and 0.1, the radial displacement reverses di-

rection — becoming inward when the flexibility ratio exceeds 2500 and 550, respectively. As the flexibility ratio becomes very large, the radial displacements approach those obtained using eq. [10a] (no lining).

Figures 8 and 9 show the normalized thrust and moment in the inner lining at the springline. Again, increasing the flexibility ratio results in a decrease in both moment and thrust. Similarly, increasing the parameter Ω also reduces moment and thrust in the inner lining. It is interesting to note that the flexibility ratio has a more pronounced influence on moments compared to thrust.

The effect of composite lining behaviour

Now, consider a composite tunnel lining comprising an inner segmental concrete tunnel lining surrounded by a thick annulus of grout and situated 13.5 m below the ground sur-

Fig. 12. Moment at the crown and the springline of the inner lining.

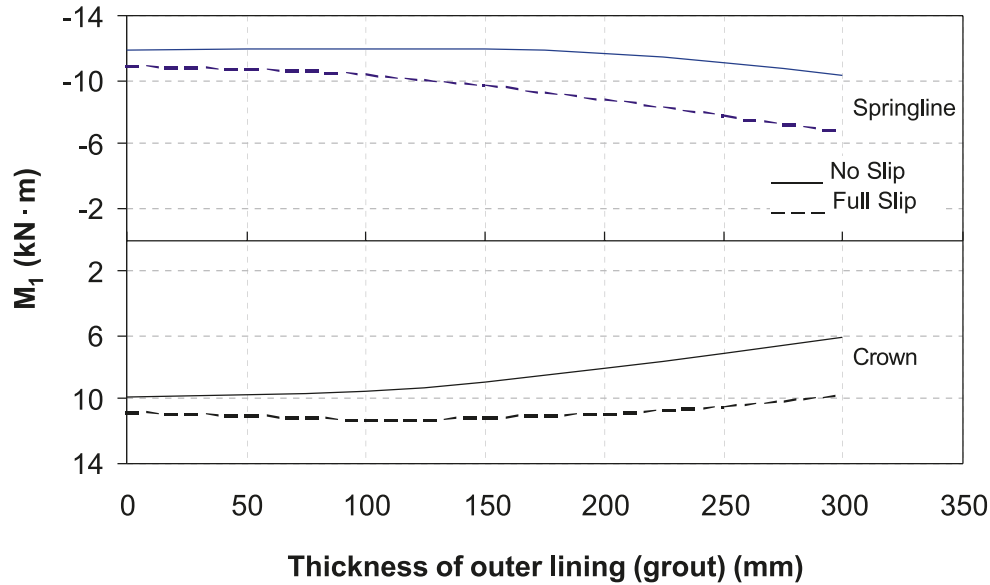
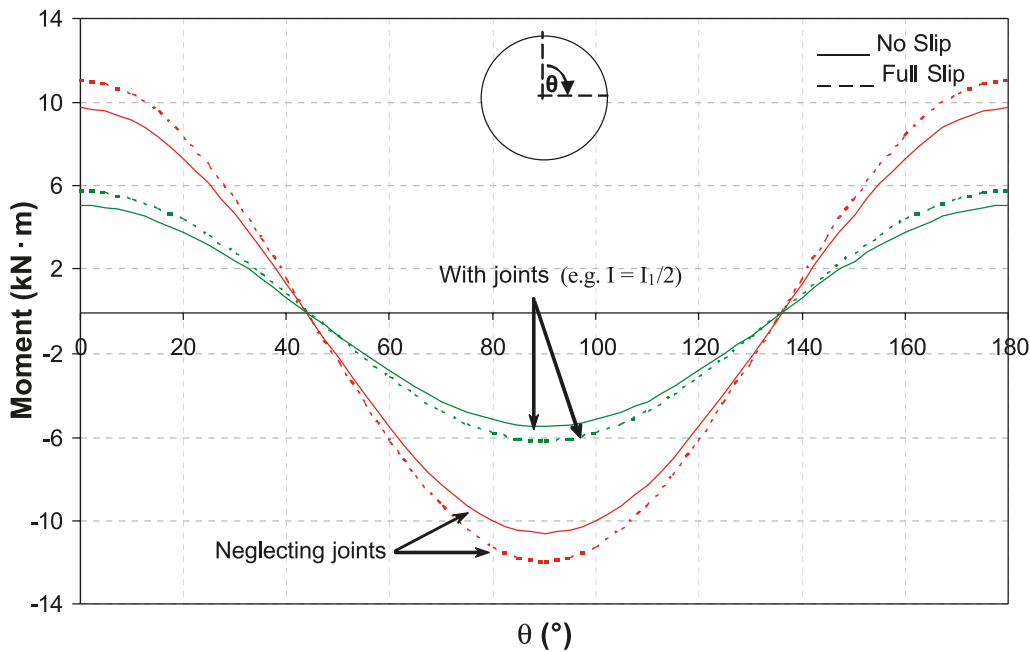


Fig. 13. Moment distribution in the inner lining for 50 mm thick grout.

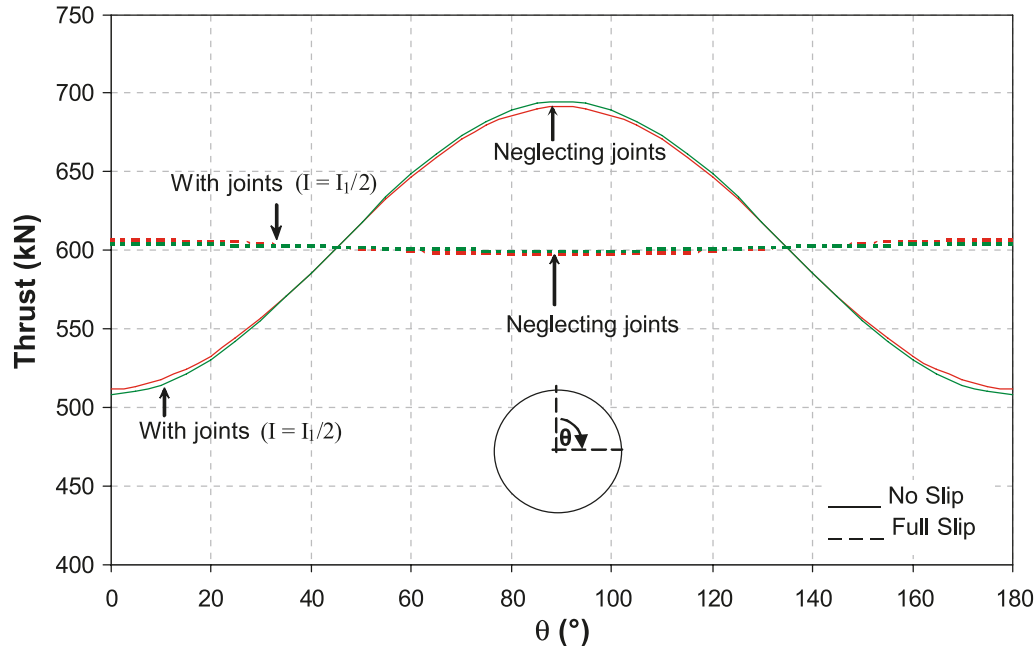


face (depth to the springline axis of the tunnel). This condition is rare, however, it has been encountered recently in Toronto, Canada and was confirmed by coring through the lining. Table 2 summarizes the soil properties assumed in the analysis. Figure 2 shows the liner geometry.

For the present analysis, it is assumed that the tunnel shown in Fig. 2 is situated above the groundwater table and embedded in a soil of sufficient strength to preclude significant plasticity in the soil mass. The inner lining is assumed to comprise a 150 mm thick precast segmental concrete lining (8 segments) with radial joints situated at the springline and crown and at 45° intervals from the springline. The inside and outside diameter of the segmental lining are 4.88 m and 5.18 m, respectively, and the liner is assumed to possess constant thickness. To illustrate composite lining behaviour,

it is also assumed that the inner lining is surrounded by a grouted annulus. Solutions for displacement, moment, and thrust of the inner lining are obtained for outer lining thicknesses, t_2 , ranging from 0 up to 300 mm. The properties of the annulus grout are summarized in Table 2. Figures 10, 11, and 12 show the effect of t_2 on the radial displacement, moment, and thrust in the inner lining neglecting the effect of the joints on the bending stiffness ($E_1 I_1$). In this case, t_2 represents the average thickness of grout since normally the grout thickness will vary around a tunnel lining. In addition, the grouted annulus would normally be neglected in design; however, it may be useful to consider the contribution of the grout when assessing the capacity of aging tunnel linings.

From Fig. 10, it can be seen that the radial displacement at the crown (inner lining) decreases as the thickness of the

Fig. 14. Thrust distribution in the inner lining for 50 mm thick grout.

outer lining increases. The impact of the outer lining is generally small, however, it becomes more predominant as the thickness exceeds about 200 mm. Figures 11 and 12, however, show the main features of the composite behaviour. From Fig. 11, the thickness of the outer lining (in this case a grouted annulus) has a pronounced effect on the magnitude of thrust in the inner lining at both the crown and springline. In contrast, the moments in the inner lining (see Fig. 12) are relatively insensitive to t_2 for the geometries considered here. From Fig. 12, it can be seen that the outer lining begins to impact in the inner lining bending moments only when t_2 reaches about 175 mm, at which point the bending stiffness of the outer and inner linings are similar.

Lastly, Figs. 13 and 14 show the distribution of moment and thrust in the inner lining accounting for the effect of joints. In this case, the impact of joints can be accounted for by reducing the moment of inertia of the inner lining in accordance with Muir Wood (1975) or Lee and Ge (2001). In Figs. 13 and 14, the moment of inertia of the inner lining has been reduced by a factor, η , of 0.5 to account for jointing. As expected, the main influence of liner joints is to reduce the moments in the lining. This is evident from Figs. 13 and 14, which show a negligible impact on thrust in the inner lining but a 48% reduction of moment at the springline.

Conclusions

In this paper, a closed-form solution has been presented for displacements, moments, and thrusts in a composite tunnel lining. In the solution, the ground is treated as an infinite elastic medium subject to an initial anisotropic stress field. The tunnel lining is idealized as an outer thick-walled cylinder and an inner thin-walled shell. In general, the solution is suitable for the analysis of composite lining systems installed in either intact rock or strong soils above the ground-

water table that remain predominantly elastic during construction of the tunnel.

The general behaviour of the solution was demonstrated for various cases involving both single and double linings. From the analysis, it is shown that the solution can be used to calculate displacements, moments, and thrusts in double linings. The solution can also be used to approximately account for such factors as jointing of the inner lining and some stress relief due to ground convergence prior to installation of the lining. In addition, a single-lining solution can be obtained by assuming that the thickness of the outer lining is very small (e.g., 0.01 m). For this condition, the solution is comparable to the Einstein and Schwartz (1979) solution. The main difference is the stress functions used to analyze the ground response. Based on the analyses and discussions presented in this paper, it is concluded that the composite lining solution is versatile, it covers several different lining geometries and conditions, and thus it should be a useful tool for design considerations in tunnelling.

Acknowledgements

The research presented in this paper has been funded by a grant from the Natural Sciences and Engineering Research Council of Canada.

References

- Einstein, H.H., and Schwartz, C.W. 1979. Simplified analysis for tunnel support. *Journal of the Geotechnical Engineering Division*, **105** (GT4): 499–518.
- Flügge, W. 1966. *Stresses in shells*. Springer-Verlag, Inc., New York.
- Lee, K.M., and Ge, X.W. 2001. The equivalence of a jointed shield-driven tunnel lining to a continuous ring structure. *Canadian Geotechnical Journal*, **38**(3): 461–483. doi:10.1139/cgj-38-3-461.

- Lee, K.M., Rowe, R.K., and Lo, K.Y. 1992. Subsidence owing to tunnelling: I Estimating the gap parameter. *Canadian Geotechnical Journal*, **29**: 929–940.
- Lo, K.Y., and Yuen, C.M. 1981. Design of tunnel lining in rock for long-term time effects. *Canadian Geotechnical Journal*, **18**: 24–39.
- Morgan, H.D. 1961. A contribution to the analysis of stress in a circular tunnel. *Géotechnique*, **11**: 37–46.
- Muir Wood, A.M. 1975. The circular tunnel in elastic ground. *Géotechnique*, **25**: 115–127.
- Ogawa, T. 1986. Elasto-plastic, thermo-mechanical and three-dimensional problems in tunnelling. Ph.D. thesis, Department of Civil and Environmental Engineering. The University of Western Ontario, London, Ont.
- Rankine, R.E., Ghaboussi, J., and Hendron, A.J. 1978. Analysis of ground-liner interaction for tunnels. Report No. UMTA-IL-06-0043-78-3, Department of Civil Engineering, University of Illinois at Urbana-Champaign, p. 441.
- Timoshenko, S.P., and Goodier, J.N. 1969. *Theory of elasticity*. 3rd ed. McGraw-Hill, New York.
- Yuen, C.M. 1979. Rock-Structure time interaction. Ph.D. thesis, Department of Civil and Environmental Engineering. The University of Western Ontario, London, Ont.

List of symbols

- θ angle measured counter clockwise from the tunnel springline
- σ_v the initial vertical stress in the ground
- σ_h the initial horizontal stress in the ground
- K'_o the coefficient of lateral earth pressure at rest
- P_o $(\sigma_v + \sigma_h)/2$
- Q_o $(\sigma_v - \sigma_h)/2$
- E_g elastic modulus of the ground
- ν_g Poisson's ratio of the ground
- E_2 elastic modulus of the outer liner
- ν_2 Poisson's ratio of the outer liner
- E_1 elastic modulus of the inner liner
- ν_1 Poisson's ratio of the inner liner
- A_1 cross-sectional area of the inner liner
- I_1 moment of inertia moment of the inner liner
- R_1 radius, inner liner intrados
- R_2 radius, inner liner extrados and outer liner intrados
- R_3 radius, outer liner extrados
- R_{cl} radius, centerline of the inner liner
- Φ Airy's stress function

- A, B, C, D constants of Airy's stress function (hydrostatic component)
- σ_R radial stress
- σ_θ tangential stress
- $\tau_{R\theta}$ shear stress
- $\Delta\sigma_R$ change in radial stress
- $\Delta\sigma_\theta$ change in tangential stress
- $\Delta\tau_{R\theta}$ change in shear stress
- ϵ_R radial strain
- ϵ_θ tangential strain
- u_g radial ground displacement
- v_g tangential ground displacement
- $u_{g \text{ react}}$ radial ground displacement due to the liner reactions
- $v_{g \text{ react}}$ tangential ground displacement due to the liner reactions
- u_{gap} radial gap displacement
- v_{gap} tangential gap displacement
- u_{L1} radial displacement of the inner liner
- v_{L1} tangential displacement of the inner liner
- u_{L2} radial displacement of the outer liner
- v_{L2} tangential displacement of the outer liner
- $\Delta D_F/D_o$ tunnel convergence at springline due to full stress relief
- $\Delta D_P/D_o$ tunnel convergence at springline due to partial stress relief
- Ω fraction of the full stress relief solution caused by convergence of the tunnel before installation of the lining
- σ_{N1}^H radial reaction between the inner and outer liners due to the hydrostatic component
- σ_{N2}^H radial reaction between the outer liner and the ground due to the hydrostatic component
- σ_{N1}^D the maximum radial reaction between the inner and outer liners due to the deviatoric component
- σ_{N2}^D the maximum radial reaction between the outer liner and the ground due to the deviatoric component
- τ_{T1} the maximum tangential reaction between the inner and outer liners due to the deviatoric component
- τ_{T2} the maximum tangential reaction between the outer liner and the ground due to the deviatoric component
- h $(R_2/R_3)^2$
- D_c compressibility constant of the inner liner
- D_f flexibility constant of the inner liner
- M moment
- T thrust

Appendix A: Equations for stresses and displacements of the outer liner

This section summarizes the solutions developed by Yuen (1979) and Ogawa (1986) for the stresses and displacements in a thick walled cylinder subject to both normal and tangential external loads.

Hydrostatic component

In a similar manner to that used for the ground, the radial, tangential, and shear stresses in the outer lining can be solved for using Airy's stress function and, eqs. [2-3a, 3b, and 3c], respectively. For the boundary conditions, $\sigma_R = \sigma_{N2}^H$ at $r = R_3$ and $\sigma_R = \sigma_{N1}^H$ at $r = R_2$, the Airy's coefficients A and C in eq. [2] are

$$[A1] \quad A = \frac{\sigma_{N2}^H - \sigma_{N1}^H h}{2(1-h)}$$

$$[A2] \quad C = \frac{R_2^2(\sigma_{N2}^H - \sigma_{N1}^H)}{(1-h)}$$

where $h = (R_2/R_3)^2$. The resultant stresses in the outer lining are

$$[A3] \quad \sigma_{R_{L2}}^H = \sigma_{N1}^H \left[\frac{(R_2/r)^2 - h}{1-h} \right] + \sigma_{N2}^H \left[\frac{1 - (R_2/r)^2}{1-h} \right]$$

$$[A4] \quad \sigma_{\theta_{L2}}^H = -\sigma_{N1}^H \left[\frac{(R_2/r)^2 + h}{1-h} \right] + \sigma_{N2}^H \left[\frac{1 + (R_2/r)^2}{1-h} \right]$$

and

$$[A5] \quad \tau_{r\theta_{L2}}^H = 0$$

From generalized Hooke's law, it can be shown that the radial displacement of the outer lining, u_{L2}^H , is

$$[A6] \quad u_{L2}^H = \int \varepsilon_{\theta_{L2}}^H dr = \frac{(1+\nu_2)r}{E_2(1-h)} \left\{ \left[-\frac{R_2^2}{r^2} - (1-2\nu_2)h \right] \sigma_{N1}^H + \left[\frac{R_2^2}{r^2} + (1-2\nu_2) \right] \sigma_{N2}^H \right\}$$

For $r = R_2$ and $r = R_3$, the radial displacements at the intrados and the extrados are

$$[A7] \quad u_{L2}^H(r = R_3) = \frac{(1+\nu_2)R_3}{E_2(1-h)} \{ [-2(1-\nu_2)h] \sigma_{N1}^H + (h+1-2\nu_2) \sigma_{N2}^H \}$$

$$[A8] \quad u_{L2}^H(r = R_2) = \frac{(1+\nu_2)R_2}{E_2(1-h)} \{ [-1 - (1-2\nu_2)h] \sigma_{N1}^H + [2(1-\nu_2)] \sigma_{N2}^H \}$$

Deviatoric component

For the deviatoric component, Q_0 , the Airy's stress function is given by eq. [6] and the radial, tangential, and shear stresses are governed by the equilibrium eqs. [7a-c], respectively. Referring to Fig. 5, the boundary conditions for the outer lining are

$$[A9] \quad \sigma_R = \sigma_{N2}^D \cos 2\theta \quad \text{at } r = R_3$$

$$[A10] \quad \tau_{R\theta} = -\tau_{T2} \sin 2\theta \quad \text{at } r = R_3$$

$$[A11] \quad \sigma_R = \sigma_{N1}^D \cos 2\theta \quad \text{at } r = R_2$$

and

$$[A12] \quad \tau_{R\theta} = -\tau_{T1}\sin 2\theta \quad \text{at } r = R_2$$

where σ_{N1}^D and σ_{N2}^D are the maximum radial stresses acting on the outer lining at the intrados and the extrados, respectively, and τ_{T1} and τ_{T2} are the maximum tangential shear stresses acting at the intrados and the extrados, respectively. Again, Fig. 5 shows the assumed stress conditions at the two interfaces.

For the above boundary conditions, the constants A , B , C , and D of the Airy's stress function are

$$[A13] \quad A = \frac{1}{2(1-h)^3} [-(2h^2 + h + 1)\sigma_{N2}^D - 2h^2\tau_{T2} + (h^3 + h^2 + 2h)\sigma_{N1}^D + 2h\tau_{T1}]$$

$$[A14] \quad B = \frac{1}{6(1-h)^3 R_3^2} [(3h + 1)\sigma_{N2}^D + (3h - 1)\tau_{T2} - (h^2 + 3h)\sigma_{N1}^D + (h^2 - 3h)\tau_{T1}]$$

$$[A15] \quad C = \frac{h^2 R_3^4}{6(1-h)^3} [-(h + 3)\sigma_{N2}^D - 2h\tau_{T2} + (3h + 1)\sigma_{N1}^D + 2\tau_{T1}]$$

$$[A16] \quad D = \frac{h R_3^2}{2(1-h)^3} [(h^2 + h + 2)\sigma_{N2}^D + (h^2 + h)\tau_{T2} - (2h^2 + h + 1)\sigma_{N1}^D - (h + 1)\tau_{T1}]$$

Using generalized Hooke's law, the radial and tangential displacements of the outer lining are

$$[A17] \quad u_{L2}^D = \int \varepsilon_r dr = \frac{2(1 + \nu_2)r}{E_2} \left[-A - 2\nu_2 B r^2 + \frac{C}{r^4} + 2(1 - \nu_2) \frac{D}{r^2} \right] \cos 2\theta$$

and

$$[A18] \quad v_{L2}^D = \int \left(\varepsilon_\theta - \frac{u_{L2}^D}{r} r d\theta \right) = \frac{2(1 + \nu_2)r}{E_2} \left[A + (3 - 2\nu_2) B r^2 + \frac{C}{r^4} - (1 - 2\nu_2) \frac{D}{r^2} \right] \sin 2\theta$$

Accordingly, the stresses and displacements at the interface between the ground and the outer lining (at $r = R_3$) due to the reactive force, σ_{N1}^D , σ_{N2}^D , τ_{T1} , and τ_{T2} are

$$[A19] \quad \sigma_{R_{L2}}^D (r = R_3) = - \left(2A + 6 \frac{C}{R_3^4} + 4 \frac{D}{R_3^2} \right) \cos 2\theta = \sigma_{N2}^D \cos 2\theta$$

$$[A20] \quad \sigma_{\theta_{L2}}^D (r = R_3) = \left(2A + 12 B R_3^2 + 6 \frac{C}{R_3^4} \right) \cos 2\theta$$

$$[A21] \quad \tau_{R\theta_{L2}}^D = \left[2A + 6 B R_3^2 - 6 \frac{C}{R_3^4} - 2 \frac{D}{R_3^2} \right] \sin 2\theta = -\tau_{T2} \sin 2\theta$$

$$[A22] \quad u_{L2}^D (r = R_3) = \frac{(1 + \nu_2) R_3}{3 E_2 (1 - h)^3} [\alpha_2 \sigma_{N2}^D + \beta_2 \tau_{T2} + \chi_2 \sigma_{N1}^D + \delta_2 \tau_{T1}] \cos 2\theta$$

and

$$[A23] \quad v_{L2}^D (r = R_3) = \frac{(1 + \nu_2) R_3}{3 E_2 (1 - h)^3} (\psi_2 \sigma_{N2}^D + \gamma_2 \tau_{T2} + \eta_2 \sigma_{N1}^D + \omega_2 \tau_{T1}) \sin 2\theta$$

where

$$\alpha_2 = (5 - 6\nu_2)h^3 + (9 - 6\nu_2)h^2 + (15 - 18\nu_2)h + (3 - 2\nu_2)$$

$$\beta_2 = (4 - 6\nu_2)h^3 + (12 - 6\nu_2)h^2 - 6\nu_2 h + 2\nu_2$$

$$\chi_2 = -4(1 - \nu_2)h(3h^2 + 2h + 3)$$

$$\delta_2 = -4(1 - \nu_2)h(h + 3)$$

$$\psi_2 = -\beta_2$$

$$\gamma_2 = -(5 - 6\nu_2)h^3 - (9 - 6\nu_2)h^2 + (9 - 6\nu_2)h - (3 - 2\nu_2)$$

$$\eta_2 = 4(1 - \nu_2)h^2(3h + 1)$$

$$\omega_2 = 8(1 - \nu_2)h^2$$

Similarly, at the intrados of the outer lining ($r = R_2$), the stresses and displacements are

$$[A24] \quad \sigma_{R_{1,2}}^D(r = R_2) = -\left(2A + 6\frac{C}{h^2R_3^4} + 4\frac{D}{hR_3^2}\right)\cos 2\theta = \sigma_{N_1}^D \cos 2\theta$$

$$[A25] \quad \sigma_{\theta_{1,2}}^D(r = R_2) = \left(2A + 12BhR_3^2 + 6\frac{C}{h^2R_3^4}\right)\cos 2\theta$$

$$[A26] \quad \tau_{R_{\theta_{1,2}}}^D(r = R_2) = \left(2A + 6BhR_3^2 - 6\frac{C}{h^2R_3^4} - 2\frac{D}{hR_3^2}\right)\sin 2\theta = -\tau_{T_1} \sin \theta$$

$$[A27] \quad u_{L_2}^D(r = R_2) = \frac{(1 + \nu_2)R_2}{3E_2(1 - h)^3} [\alpha_1 \sigma_{N_2}^D + \beta_1 \tau_{T_2} + \chi_1 \sigma_{N_1}^D + \delta_1 \tau_{T_1}] \cos 2\theta$$

and

$$[A28] \quad v_{L_2}^D(r = R_2) = \frac{(1 + \nu_2)R_2}{3E_2(1 - h)^3} [\psi_1 \sigma_{N_2}^D + \gamma_1 \tau_{T_2} + \eta_1 \sigma_{N_1}^D + \omega_1 \tau_{T_1}] \sin 2\theta$$

where

$$\alpha_1 = -\chi_2/h$$

$$\beta_1 = \eta_2/h$$

$$\chi_1 = -(3 - 2\nu_2)h^3 - (15 - 18\nu_2)h^2 - (9 - 6\nu_2)h - (5 - 6\nu_2)$$

$$\delta_1 = -2\nu_2h^3 + 6\nu_2h^2 - (12 - 6\nu_2)h - (4 - 6\nu_2)$$

$$\psi_1 = \delta_2/h$$

$$\gamma_1 = -\omega_2/h$$

$$\eta_1 = -\delta_1$$

$$\omega_1 = (3 - 2\nu_2)h^3 - (9 - 6\nu_2)h^2 + (9 - 6\nu_2)h + (5 - 6\nu_2)$$